Joint Angle Control by FES Using a Feedback Error Learning Controller

Kenji Kurosawa, Ryoko Futami, Takashi Watanabe, *Member, IEEE*, and Nozomu Hoshimiya, *Fellow, IEEE*

Abstract—The feedback error learning (FEL) scheme was studied for a functional electrical stimulation (FES) controller. This FEL controller was a hybrid regulator with a feedforward and a feedback controller. The feedforward controller learned the inverse dynamics of a controlled object from feedback controller outputs while control. A four-layered neural network and the proportional-integral-derivative (PID) controller were used for each controller. The palmar/dorsi-flexion angle of the wrist was controlled in both computer simulation and FES experiments. Some controller parameters, such as the learning speed coefficient and the number of neurons, were determined in simulation using an artificial forward model of the wrist. The forward model was prepared by using a neural network that can imitate responses of subject's wrist to electrical stimulation. Then, six able-bodied subjects' wrist was controlled with the FEL controller by delivering stimuli to one antagonistic muscle pair. Results showed that the FEL controller functioned as expected and performed better than the conventional PID controller adjusted by the Chien, Hrones and Reswick method for a fast movement with the cycle period of 2 s, resulting in decrease of the average tracking error and shortened delay in the response. Furthermore, learning iteration was shortened if the feedforward controller had been trained in advance with the artificial forward model.

Index Terms—Controller, feedback error learning (FEL), functional electrical stimulation (FES), neural network.

I. INTRODUCTION

FUNCTIONAL electrical stimulation (FES) is an advancing technology for restoring paralyzed motor functions caused by a spinal cord injury or a stroke. It applies programmed electrical stimuli to intact peripheral nerves or muscles. One important research subject on FES is the development of adequate controllers for determining an appropriate time course of stimuli, which is necessary for restoring desired functional movements, such as grasping, walking, and so on. Accurate and stable control of limbs by FES is a very difficult subject because electrically stimulated musculoskeletal systems have strong nonlinearity [1], time variability, large latency and a time constant, and fatigue [2] in their response. Furthermore, the controllers must solve ill-posed problems because the number of muscles is generally greater than the degrees of freedom (DOFs) of limbs.

Many control strategies have been proposed in the literature. They are categorized fundamentally into several types: open loop [3]–[7], closed-loop [8]–[12], their hybrid controllers [13]–[17], and rule-based controllers [18], [19]. Stimulation patterns were generated using lookup-tables [3], [4], [20], [21], mathematical models [9], [22], artificial neural networks [5], [7], [13], [14], [23], the PID or its simplified controllers [8], [10]–[12], [24], fuzzy controllers [15], [25], [26], etc. Not only controllers with fixed parameters, but also adaptive controllers have been studied for FES applications [13], [15], [26]–[28].

The open-loop control scheme is often preferred at clinical sites because of its simplicity. However, open-loop controllers need initial and periodical adjustment in stimulation patterns for individual patients, which must be done by medical doctors. These adjustments are time-consuming, burdening both patients and medical staff. Moreover, open-loop controllers cannot eliminate effects of disturbances such as external loads and muscle fatigue. Closed-loop control systems are superior to open-loop systems to compensate disturbance and control stabilization [8], [12]; however, the control systems require appropriate sensors. The authors showed that the proportional-integral-derivative (PID) controller, which was improved to deal with redundant musculoskeletal systems, performed accurate tracking on trajectory tracking tasks of the wrist joints' two DOF movements [24]. However, the tracking error increased as the velocity of the desired movement increased because the latency and the time constant in the response of the musculoskeletal system were not negligible for the fast movement. The control tends to be late or oscillatory as a result of the large time lag in the musculoskeletal systems that occurs when the closed-loop controllers try to regulate stimuli after control errors are detected. From the viewpoint of patient safety and accuracy of control, the control delay can be undesirable for FES applications.

The hybrid controllers are expected to incorporate advantages of both feedforward and the feedback controllers: the feedforward controllers enable fast movements without delay, whereas the feedback controllers are able to compensate for disturbance. Chang *et al.* [14] showed that the control delay with a neuro-PID controller was smaller than that with the PID controller for evaluation of knee-joint position control. However, most hybrid controllers proposed in the literature required initial adjustment or learning of the feedforward controllers before they could be used to control limbs. Therefore, the burden of these adjustments of feedforward controllers remained even in those control schemes. Moreover, few hybrid controllers were evaluated on redundant musculoskeletal systems.

This study adopts a feedback error learning (FEL) scheme [29]–[31] into an FES controller [32]. The FEL controller is regarded as a hybrid controller combining the feedforward and the feedback controller. The important thing is that the feedforward controller learns the inverse dynamics of controlled limbs from outputs of the feedback controller during the control of limbs. The inverse dynamics is the inverse function of the transfer function of FES-controlled limbs. If the feedforward controller acquires the inverse dynamics, it can generate appropriate stimuli for given desired movements. Self-adaptation process of the feedforward controller for the purpose of acquiring the inverse dynamics is called "learning" in this paper. Although appropriate sensor systems are required, the FEL controller is expected to simplify and shorten the clinical adjustment tasks because it does not need separating learning and control phase. Furthermore, the FEL controller is able to control redundant musculoskeletal systems if the feedback component in the FEL controller can deal with such redundant systems. This paper presents adoption and evaluation of the FEL controller on FES induced 1–DOF joint angle controls in both computer simulations and FES experiments. One extensor group and one flexor of able-bodied subjects were co-stimulated. Therefore, the controller had to solve an ill-posed problem because the controller received one input (desired joint angle) and provided two outputs (stimulus currents).

Controller parameters were optimized in computer simulation with a forward dynamics model of the wrist that can be used as a controlled object. The forward dynamics model was prepared by training an artificial neural network to imitate the response of the subject's wrist angle to electrical stimulation. The wrist was selected herein as a controlled object because the authors had studied on upper extremity FES for C4 patients [3] and accurate control of each joint including the wrist can be an important research subject for sophisticated multijoint upper extremity FES. The methodology presented in this paper is not specialized for the wrist, and it can be used for FES-induced controls of other joints including lower extremities.

Subsequently, we will show that the FEL controller performed better than the conventional PID controller adjusted by the Chien, Hrones, and Reswick (CHR) method in evaluation of delay time and tracking error for fast movements (2 s cycle period) on FES experiments with six able-bodied subjects. Furthermore, we will show that the learning period of the feedforward controller (Inverse Dynamics Model; IDM) in the FEL controller can be shortened when it is trained in advance with the forward dynamics model.

II. METHODS

This chapter describes the proposed controller and experimental methods. After description of the controller (Section II-A), Sections II-B–II-D present the experimental methods. Fig. 1 shows the flow chart of the experiments. First of all, the joint angle responses of subjects are measured with ramp, step, and random stimulation patterns. The data are used to determine parameters in the feedback component (Section II-A) and to train a forward dynamics model (Section II-B). Then, other controller parameters are optimized
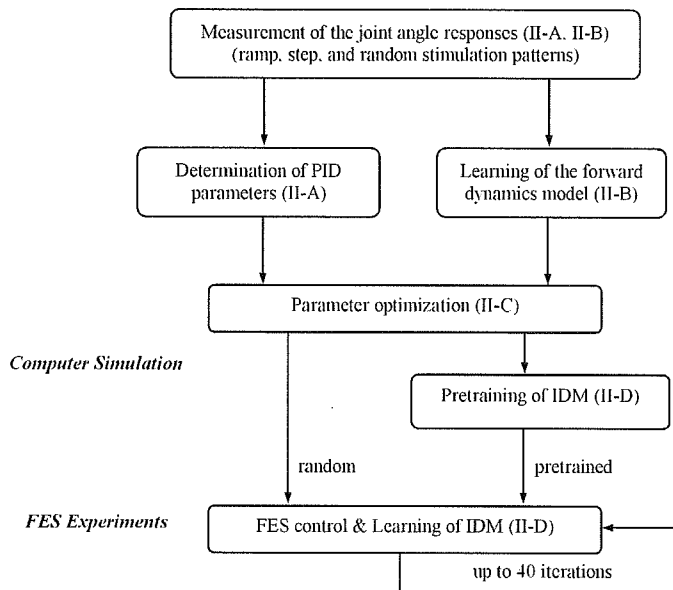

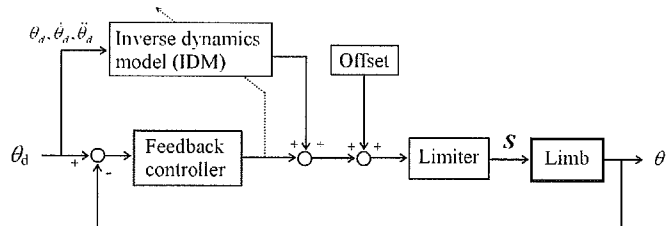Fig. 1. Flowchart of experiments. Details are explained in each section ("II-A" means Section II-A).

Fig. 2. Block diagram of the control system. θ_d, θ, and S represent the desired joint angle, the measured joint angle, and the stimulus current vector, respectively. The controller has a hybrid arrangement of a feedforward (inverse dynamics model; IDM) and a feedback controller. IDM learns from the output of the feedback controller while controlling limbs.

in computer simulation (Section II-C). Afterwards, iterative FES experiments will be done with the optimized parameters (Section II-D). Six able-bodied subjects' wrists are controlled in two situations. One is the situation when the wrist angle is controlled iteratively after connection weights in the feedforward controller (a neural network) are determined by a random number generator. The other situation is when it is controlled iteratively after the feedforward component is pretrained in computer simulation.

A. Feedback Error Learning FES Controller

1) General Description: Fig. 2 shows a block diagram of the control system. The FEL controller has a hybrid arrangement of a feedforward (inverse dynamics model; IDM) and a feedback controller. Thus, the FEL controller incorporates both the advantages of the nonlinear dynamics given by the feedforward component and the disturbance compensation ability by the feedback component. In general, both IDM and an inverse kinematics model (IKM) are required to form an inverse model; however, IKM is left out herein because this paper addresses single joint control. In addition, IDM learns the inverse dynamics of controlled limbs from the outputs of the feedback controller while controlling them. Therefore, both the control and learning of IDM are carried out at the same time. For that
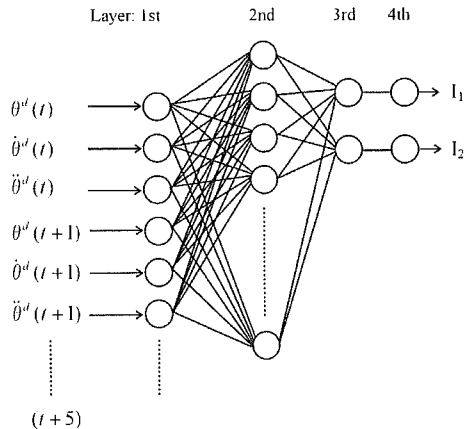
Fig. 3. Structure of the IDM. Inputs are the desired joint angle and their first- and second-order derivatives at times t to $t+5$. Outputs are stimulus currents to each muscle. Number of neurons in the second layer is determined in computer simulation.

reason, it is not necessary to divide the control phase and the learning phase. The feedback controller functions mainly when IDM is not learned, then the role gradually transits to IDM as learning progresses. This means that IDM mainly controls limbs and the feedback controller functions as a disturbance compensator if IDM acquires the inverse dynamics of limbs perfectly.

The input signal is the desired joint angle (θ_d), and IDM outputs stimulus current to each muscle as the feedforward controller using the desired angle and its first and second derivatives. The feedback controller also outputs stimulus current for each muscle to cancel out the difference between the desired joint angle (θ_d) and the actual angle (θ). The summed vector of the respective controllers' outputs and the offset corresponding to the threshold levels of electrically stimulated muscles is determined as the FEL controller output (S), after clipping out with the limiter to prevent excessive stimulation. In general, the controller must solve the ill-posed problem because the dimension of S is higher than that of θ.

2) Feedforward Controller: In this study, a four-layered perceptron (Fig. 3) was used to form IDM. The inputs were the desired angle, angular velocity, and angular acceleration at the time t to $t+5$. One discrete time interval corresponds to 50 ms. Therefore, the desired trajectory at the present time and the near future (until 250 ms later) was given to IDM. The output of each neuron was defined as

$$y = f\left(\sum_i w_i x_i + c\right) \tag{1}$$

where x_i represents outputs of the neurons in the previous layer, w_i are the connection weights from neurons in the previous layer, c is the bias term, and i is the index of the neuron in the previous layer. This is a common expression of an artificial neuron model. The output function $f(x)$ of the neurons in the second and the third layers is the sigmoid function

$$f(x) = \frac{1}{1 + e^{-x}}. \tag{2}$$

The output range of this function is 0–1 because x is a real number. The output function in the fourth layer is linear as

$$f(x) = x. \tag{3}$$

The error back-propagation algorithm [33], [34] was used for IDM learning. The learning rule is to change the connection weights so as to reduce total error (E) in the network outputs by gradient descent

$$\Delta w_i = -\varepsilon \cdot \frac{\partial E}{\partial w_i}. \tag{4}$$

The coefficient ε is the learning speed coefficient that effects on convergence speed of learning. The outputs of the feedback controller were referred as error signals. The connection weights were adjusted between the first and the second layer, and between the second and the third layer. The connection weights between the third and the fourth layer were fixed at ($I^i_{\max}-I^i_{th}$), and the bias terms in the fourth layer were fixed at zero. The values of $I^i_{\max}$, I^i_{th} describe the maximum and the threshold current of muscle i, respectively. The outputs of IDM were feedforward stimulus currents to each muscle.

3) Feedback Controller: The PID controller given by (5) was used as the feedback component

$$I_n = K_P e_n + K_I \sum_{i=0}^n e_i + K_D(e_n - e_{n-1}). \tag{5}$$

In (5), the error vector e_n was defined as $e_n = \theta_n^{(D)} - \theta_n^{(M)}$ ($\theta_n^{(D)}$, $\theta_n^{(M)}$ are the desired and the measured joint angle vector at time n). The CHR method [35] was used to determine the PID parameter matrices K_P, K_I, and K_D with the following two criteria; quick response without overshoot, and step change in the desired value. Because the original CHR method was proposed on single–input, single–output (SISO) systems, we applied it on single–input, multiple–output (SIMO) systems as follows:

$$K_{Pij} = \frac{0.6T_i}{L_i} m^-_{ij}, K_{Iij} = \frac{0.6\Delta t}{L_i} m^-_{ij}, K_{Dij} = \frac{0.3T_i}{\Delta t} m^-_{ij} \tag{6}$$

where L_i and T_i are the latency and time constant of the step response of muscle i, and Δt is the sampling period. Coefficients m^-_{ij} transform the joint angle space into the stimulus current space. In this paper, the coefficients were elements of a generalized inverse matrix of the Jacobian matrix M describing the relationship between stimulus current vectors and joint angle vectors of a musculoskeletal system [24].

B. Development of a Forward Dynamics Model of the Wrist

We developed a forward dynamics model of the wrist that can be used in computer simulations for optimizing controller parameter. Two muscles were selected for the dynamics model; their responses in the palmar/dorsi- flexion angle were modeled. The muscles were the extensor carpi radialis longus/brevis (ECR: ECRL and ECRB) and the flexor carpi ulnaris (FCU). Because selective stimulation was difficult with surface electrodes, the extensor carpi radialis longus and the extensor carpi radialis brevis were treated as a single muscle and labeled as ECR in this paper.

The forward dynamics model was composed, as shown in Fig. 4, using artificial neural networks. The dynamics model consisted of two components: a static nonlinear part and a part expressing second-order dynamics. Two circuits were prepared for gravitational and for anti-gravitational movements in the dynamics component because the time constant differed between
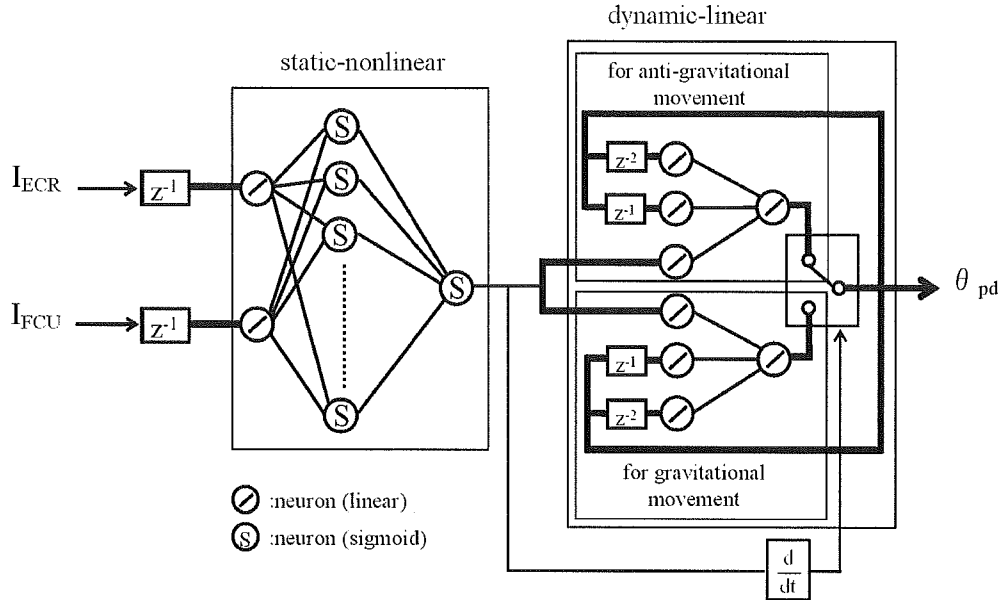
Fig. 4. Structure of the forward dynamics model. Inputs are the stimulus currents to ECR and FCU, followed by the one-tap delay (z^{-1}). Output is the wrist angle in the direction of dorsi/palmar flexion. Model comprises two components: static–nonlinear and dynamic-linear components. Latter describe linear and second-order dynamics, in which two circuits are prepared for anti-gravitational and gravitational movements. Circuits are switched according to the direction of movements. Connection weights of the thick connections are unity. Only the thin connections are adjusted by the error back-propagation algorithm.

these movements. Two types of neurons were included in the network. The first kind were neurons of which output function was the sigmoid function given by

$$f(x) = \frac{1 - e^{-x}}{1 + e^{-x}} \qquad (7)$$

whereas other neurons had a linear output function as in (3).

The connection weights in the network shown as thick lines were unity, whereas those shown as thin lines were adjusted by the error back-propagation algorithm. The teacher signals were obtained from an able-bodied subject (Subject A) who had sufficient experience with surface electrical stimulation. Ag/AgCl surface electrodes (F-150M; Nihon Koden Corporation) were placed over the motor points of the muscles in his left forearm. The stimulation frequency and the pulse width were fixed at 20 Hz and 200 μs, whereas the pulse amplitude (current) was modulated. The subject sat on a chair with his left arm hanging to the gravitational direction (down); the shoulder, the elbow, and the hand were in a free position. Thereby, the forearm was about 90° pronated from the anatomical position. The subject was instructed to relax his left arm and hand as much as possible. The neutral angle of the wrist was defined at this posture.

Fifty-eight stimulation patterns (12: ramp shaped patterns, 6: step, and 40: random) were applied to the subject. The random patterns were produced by filtering random time series with the Butterworth-type low-pass filter whose cutoff frequency was 1 Hz. The joint angle was sensed with a magnetic three-dimensional (3-D) position and orientation sensor (FASTRAK; Polhemus Inc.). The measured response data were used as teacher signals for the purpose of learning of the forward dynamics model. For random patterns, only 20 patterns were used for learning. The remaining 20 patterns were used for validation of the forward model. Learning was done in two steps: learning of the static part, then learning of the dynamic parts.

C. Computer Simulation

1) Parameter Optimization: The forward dynamics model described in the previous section was used as a controlled object in this simulation study. This computer simulation was intended for parameter optimization, e.g., the number of the neurons in the hidden layer of IDM and the learning speed coefficient (ε).

Clinical-site use of the FEL controller demands that iterations and the time required for IDM learning should be minimal without sacrificing learning stability. Therefore, the learning speed coefficient was set large (0.0003 for the desired trajectory explained in the following paragraph) at the beginning of the learning. Afterwards, it was halved as learning progressed for the purpose of fine-adjustment of the connection weights. Initial connection weights in IDM were determined by a random number generator, which was regulated so that the unlearned IDM did not produce large outputs.

Our previous experimental results [24], which concerned the trajectory tracking control of the wrist by the PID controller that could deal with redundant musculoskeletal systems, showed that the control error was largely the result of delayed response that occurred when the cycle period of the desired trajectory became fast (3 s). In this study, the controller was evaluated at a faster movement with the cycle period of 2 s (0.5 Hz). The trajectory was ten reciprocating sinusoidal motions of 50° in amplitude (15° in the palmar-flex, 35° in the dorsi-flex). These ten reciprocating motions constituted one iteration when IDM learned.

The progress of IDM learning was demonstrated by computer simulation when the number of neurons in the second layer varied from 9 to 72. These numbers were a half to four times the number of neurons in the first layer. Simulation was carried out 100 times for each condition; the initial connection weights were regenerated by the random number generator at the beginning of each trial.

2) Evaluation on Other Trajectories: The same FEL controller was used for controlling and learning other movements. The trajectories were three sinusoidal movements (the cycle period was 1 s, 4 s, and 10 s) and a random movement. The random trajectory was produced by filtering random time series with the Butterworth-type low-pass filter whose cutoff frequency was 0.75 Hz. The number of neurons in the second layer was 36, and the initial value of the learning speed coefficient was 0.0003. The computer simulation was done four times for each trajectory.

D. FES Experiments

After the computer simulations, the controller was evaluated on FES experiments with six able-bodied subjects (Subject A–F). Able-bodied subjects were used for this study because they were more readily available and because, in general, a relaxed able-bodied limb and a paralyzed limb respond similarly to electrical stimulation [14], [39]. However, there are significant differences between normal and paralyzed limbs (e.g., spasticity of paralyzed limbs). Therefore, results presented in this paper will be referred on FES controls of limbs not exhibiting spasticity. The subjects were checked during experiments whether or not they were relaxed their forearm and hand by giving sudden stops of electrical stimuli without previous notice and by observing the response movements. In addition, the subjects were not given any information about experimental conditions such as a desired trajectory to avoid intentional voluntary contractions.

The palmar/dorsi-flexion angle was controlled by contracting ECR (ECRL and ECRB) and FCU. The stimuli were delivered to the peripheral nerves of the muscles in their left forearm with a pair of Ag/AgCl surface electrodes (F-150M; Nihon Koden Corporation) placed over the motor points. A laboratory FES system incorporating a 3-D position-orientation measurement system (FAS-TRAK; Polhemus Inc.) was used to generate pulse stimuli and to measure the wrist angle [37]. The 3-D position-orientation measurement system was used for sensing the joint angle. It consists of a fixed magnetic-dipole transmitting antenna called a transmitter (5.3 × 5.3 × 5.8 cm, 0.27 kg), freely movable magnetic-dipole receiving antennas called receivers (2.83 × 2.29 × 1.52 cm, 17.0 g), and a System Electronics Unit (28.91 × 28.90 × 9.22 cm, 2.26 Kg). The system calculates 3-D position and orientation of the receivers in the transmitter coordinates using electro-magnetic fields. The static accuracy is 0.08 cm root means square (rms) for the receiver position and 0.15° rms for the receiver orientation, when the receivers are placed within 76 cm from the transmitter. In our experiments, the transmitter was placed and fixed near the subjects, and two receivers were placed on the subjects to sense the wrist angle: one was on the back of the hand, and the other one was on the back of the forearm close to the wrist. The wrist angle can be obtained only using the orientation data of the receivers by calculations of rotational matrices [37]. The system was developed for laboratory use.

The pulse amplitude was modulated at the range of 0–25 mA, whereas the pulse width and the frequency were fixed at 200 μs and 20 Hz, respectively. The desired trajectory was ten sinusoidal reciprocating motions with the cycle period of 2 s (0.5 Hz) to evaluate the control performance for the faster movement containing single frequency. The able-bodied
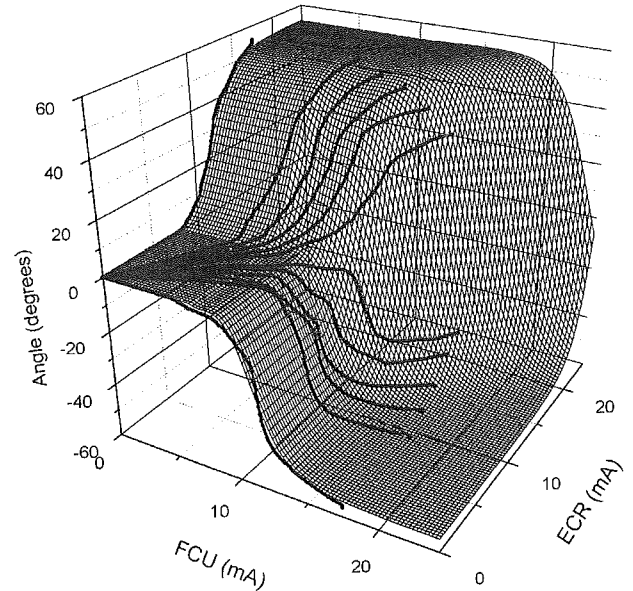

Fig. 5. Static responses of the model output (mesh) and subject's wrist (lines).

subjects might recognize that the reference trajectory was sinusoidal movement after a few iterations. However, it was expected that this did not affect evaluation of delay time and tracking error because the subjects had no information about the exact start timing and the amplitude of the desired movement. Learning-control activities were performed up to 40 iterations. The subjects seated with his left arm hanging; the shoulder, the elbow, and the hand were in a free position. Thereby, the forearm was about 90° pronated from the anatomical position. The neutral angle of the wrist was defined at this posture.

The number of neurons in the second layer of IDM was 36; other parameters, such as the learning speed coefficient, were the same optimized values determined in the computer simulations. Control performance was evaluated with the mean absolute error and the delay time. These FES experiments were done in three situations: the FEL controller whose initial weights in IDM were determined by a random number generator (random), the FEL controller in which IDM was pretrained in advance with the forward dynamics model in computer simulation (pretrained), and the PID-only control (pid). The PID parameters were determined by the CHR method. Experiments were done three times on different days for Subject A, whereas a single time for Subject B–F; total eight sets for the six subjects.

Effect of an external load on control performance was also tested with one subject (Subject A). After learning of IDM under the load-free condition, a 250 g ceramic cup was fastened to the hand with a brace. Then, the wrist angle was iteratively controlled with the FEL controller. The desired trajectory was the same ten sinusoidal reciprocating motions with the cycle period of 2 s.

III. RESULTS

A. Forward Dynamics Model of the Wrist

Outputs from the learned forward model were compared with measured responses. Fig. 5 shows static characteristics. The x and y axes represent stimulus currents applied to each muscle,
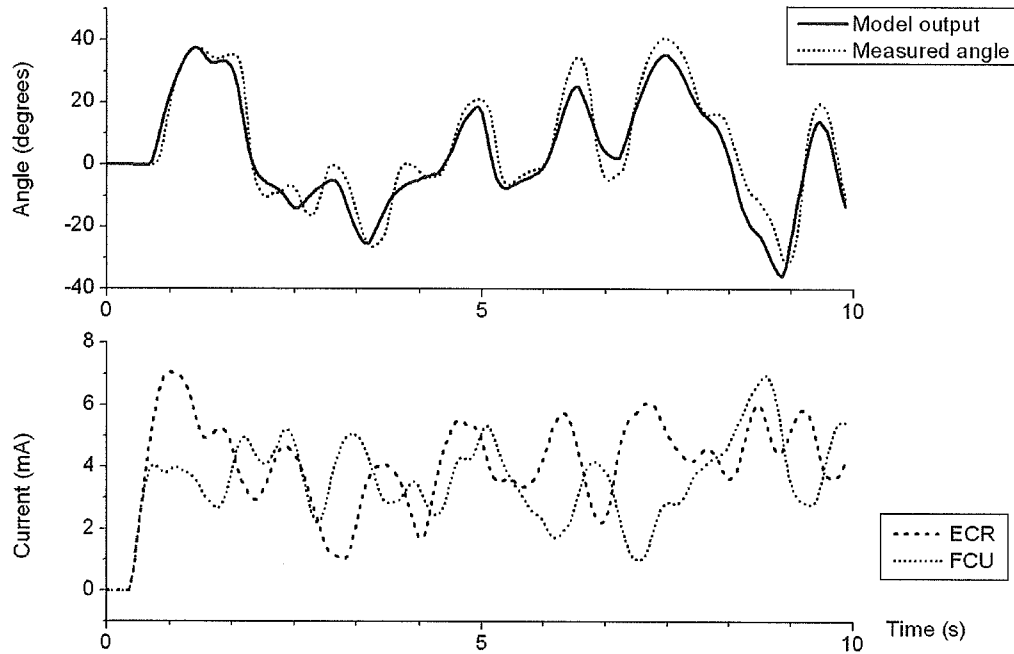
Fig. 6.   Example of the dynamic response to the random stimulation pattern. Upper graph shows the model output and the measured angle of the subject's wrist. Mean error was 4.5°. Lower graph shows the stimulation pattern.

whereas the z-axis shows the joint angle. The measured characteristic was drawn with thick lines, which were superimposed on the mesh that shows the model outputs. The mean error between the measured angle and the model output for all 12 lines was 1.8° and the standard deviation was 0.5°. Fig. 6 shows a dynamic response to a random stimulation pattern that was not used for learning. The upper graph shows the model output and the measured actual angle when the stimulation pattern shown in the lower graph was applied. The mean error and the standard deviation of the 20 random patterns used for the learning were 4.9°, and 1.6°, whereas the values of the other 20 random patterns that were not used for the learning were 5.6°, and 1.7°, respectively. The mean error was 2.7° and the standard deviation was 0.8° for six-step stimulation patterns. For all 58 patterns including both static and the dynamic responses, the mean error was 4.3° and the standard deviation was 2.0°. These results indicate that the forward dynamics model successfully acquired the characteristics of the subject's wrist. Thus, this model was controlled in the computer simulations.

B. Computer Simulation

1) Parameter Optimization: The number of neurons in the second layer was determined in the computer simulation after optimization of the learning speed coefficient and distribution range of initial connection weights in IDM. The mean tracking error as a function of the iteration number is plotted in Fig. 7. Two typical cases from the 100 trials for each condition are shown in the graph. Fast convergence of the error was usually observed when the number of the neurons was 18 or 36. The graph shows that the error became small as the iteration number and the learned FEL controller performed better than the PID controller adjusted by the CHR method because tracking error by the PID was 7.1°. The average error decreased because of shortened delay in the response. The percentage of successful
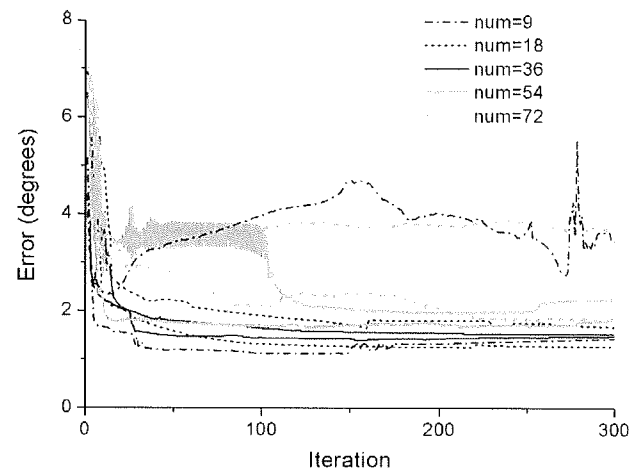

Fig. 7.   Mean tracking error as the function of the iteration number. Number of the neurons in the second layer (num) was varied in the range of 9–72. If the PID controller was used alone, the error was 7.1°. Two typical cases from the 100 trials for each condition are shown.

TABLE I
PERCENTAGE OF SUCCESSFUL LEARNING

Number of neurons in the 2nd layer	Percentage (%)
9	70
18	96
36	90
54	47
72	29

learning is presented in Table I. The successful learning was judged according to whether or not the average tracking error fell to less than 2.5° at the 50th iteration. It was shown that the percentage exceeded 90% for 18 or 36 neurons. The percentage fell when the number was larger or less than these values.
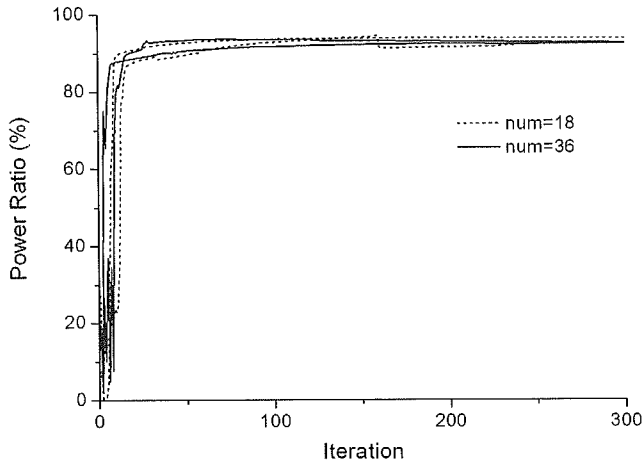
Fig. 8. Change of the power ratio as the function of the iteration number. Number of the neurons in the second layer (num) was 18 or 36. When the power ratio was 0%, it describes that only the PID controller functioned. About 90% of the control was held by IDM after the 20th iteration. Two typical cases from the 100 trials for each condition are shown.

Fig. 8 shows the change of the power ratio in the FEL controller defined as follows:

$$\text{Power ratio}(\%) = \frac{\sum P_{\text{IDM}}(t)}{\sum P_{\text{PID}}(t) + \sum P_{\text{IDM}}(t)} \times 100. \qquad (8)$$

Here, $P_{\text{IDM}}(t)$ represents the output power of IDM at time t, whereas $P_{\text{PID}}(t)$ is the power of the PID controller. Fig. 8 shows that the wrist was controlled mostly by the PID controller at the first iteration; thereafter, IDM became the dominant controller within 20 iterations in most trials. This demonstrated that IDM successfully learned the inverse dynamics of the forward model because the power ratio was high and the joint angle was controlled with small average error.

2) Evaluation on Other Trajectories: The controller was applied for other trajectories. The number of neurons in the second layer was 36. Fig. 9 shows the change of the average tracking error for each sinusoidal movement. Fast convergence of the error was usually observed when the cycle period (T) was 2, 4, and 10 s. In general, the error decreased as T increased. However, fast convergence of the error was not observed for $T = 1$ s. The learning failed for $T = 1$ even though the number of neurons and other controller parameters were varied. Saturation of stimulus currents was observed in these failed learning. These simulation results show that the learning of IDM will succeed when desired trajectories have frequency bands of 0.5 Hz or lower.

Fig. 10 shows an example of control performance for a random trajectory. Fig. 10(a) shows the time course of the joint angle. A typical result is drawn. The dotted line showing "before learning" was the result of the first iteration, whereas "after learning" was the result of the 100th iteration. Delay in the response was observed in the result of "before learning." The response delay remarkably decreased "after learning." However, quick motions were observed around inflection points in the desired trajectory.

Fig. 10(b) shows the change of the average tracking error and the power ratio as a function of the learning iteration. The simulation was done four times for the same random reference trajectory. Transition of the dominant controller from the PID to IDM was observed in most trials because the power ratio changed
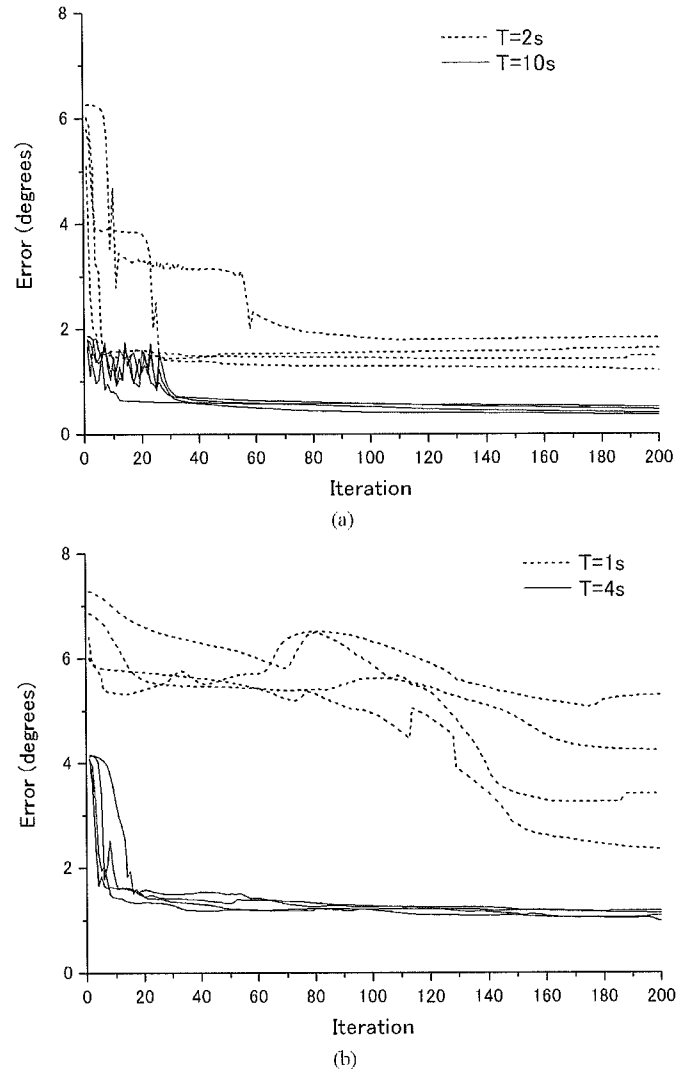

(a)

(b)

Fig. 9. Mean tracking error as the function of the iteration number. Number of the neurons in the second layer was 36. Desired trajectories were ten reciprocating movements with the cycle period (T) of 1, 2, 4, and 10 s. Computer simulation was done four times for each cycle period.

from 0%–20% to 85%–90%. The average tracking error halved after learning as the delay time decreased.

C. FES Experiments

The FEL controller worked as expected in all FES experiments for all subjects. Fig. 11 shows examples of control performance when the experimental condition was "random." Graphs in Fig. 11(a) show the result of the first iteration (i.e., first control just after the connection weights in IDM were determined by the random number generator). If the PID controller was used alone, the results were almost identical to this result. Fig. 11(b) shows the 32nd iteration result. Fig. 11(a), the time course of the joint angle, Fig. 11(b) the tracking error, Fig. 11(c) the stimulus currents, and Fig. 11(d) the outputs of each controller are shown. The muscles were co-contracted when the joint angle crossed 0°; the threshold of the stimulus current for ECR was 7.0 mA and that for FCU was 5.1 mA. As for the first iteration [Fig. 11(a)], small amplitude and large delay in the response were observed. IDM generated small outputs and the joint angle was mostly controlled by the PID controller as seen

(a) Time course of the joint angle
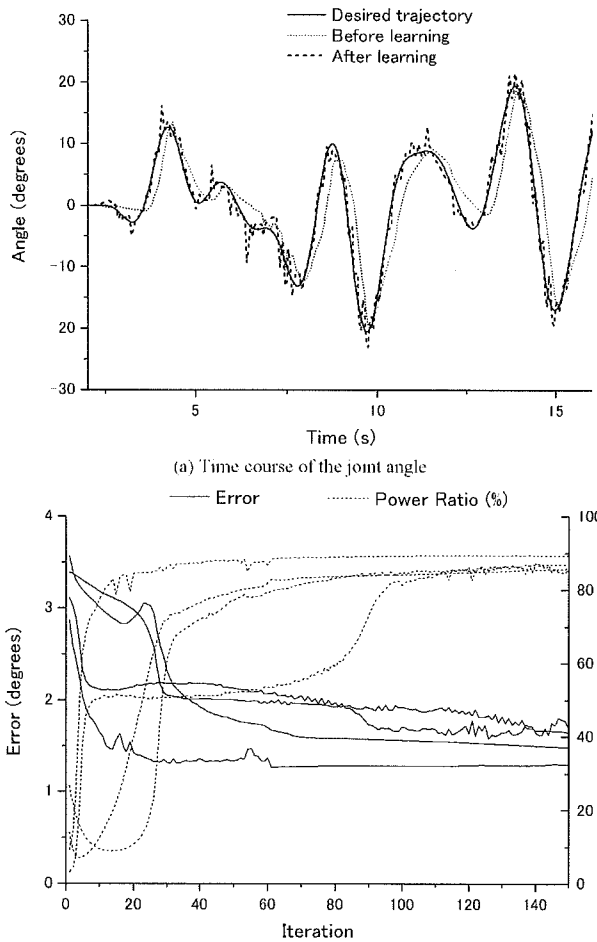
(b) Change of the average error and the power ratio as a function of the learning iteration

Fig. 10. Computer simulation results for a random trajectory. Random trajectory was produced by filtering random time series with the Butterworth-type low-pass filter whose cutoff frequency was 0.75 Hz. (a) Time course of the joint angle. A typical result is drawn. Dotted line showing "after learning" is the result of the 100th iteration. (b) Change of the average error and the power ratio. Computer simulation was done four times for the same random trajectory. If the PID controller was used alone, the error was 3.7°.

in the bottom graph. The delay decreased remarkably and the tracking error became small after 32 times iterative learning as shown in Fig. 11(b) even though small oscillatory motion was seen when the angle changed from plus (dorsi-flex.) to minus (palmar-flex.). Furthermore, primary output was produced by IDM as shown in the bottom graph. These results demonstrated that the control performance improved because IDM successfully acquired inverse characteristics of the subject's wrist. It must be noticed that the amplitude in the response movement shown in Fig. 11(a) could be enlarged if the PID parameter matrixes were optimized for this specific trajectory. However, the authors determined the parameters by the CHR method because the parameters could be obtained systematically with simple procedures. Moreover, it was thought difficult to decrease response delay without oscillations just by adjusting the PID parameter matrixes.

Fig. 12 shows the results when IDM was pretrained with the forward dynamics model in computer simulation (pretrained). The subject (Subject F) was a different person who cooperated in development of the forward dynamics model. The re-

sponse delay and the error were small from the first iteration although the palmar-flex. angle was short to the desired trajectory [Fig. 12(a)]. Moreover, it was seen that IDM produced large outputs. Adding a few iterations of electrical stimulation, the control performance improved and the outputs of the PID controller became small as shown in Fig. 12(b).

Fig. 13 shows changes in the average error and the power ratio defined by (8). The error decreased to about 40% of the first iteration and the power ratio increased as iterations proceeded. The change of the power ratio indicated the transition of the dominant controller from the PID to IDM. About 80% of the control was held by IDM after the 18th iteration. The thick solid and dashed lines show the error and the power ratio if IDM was pretrained. The error was small and the power ratio was high from the first iteration. Adding a few iterations of electrical stimulation, about 90% of the control was held by IDM with small average error. The result demonstrated that the iteration and the time required for learning of IDM could be shortened with pretraining. This result has great implications for clinical applications.

Fig. 14 summarizes the average delay time and error of all FES experiments for six subjects. The delay time was calculated by averaging ten data at the 5° in dorsi-flexion (i.e., the phase angles in the trajectory were 0 rad, and π rad). The delay time and the error for "pid" (i.e., when only the PID controller was used) were almost identical to the values for "random (before learning)" because IDM generated small outputs and the dominant controller was the PID in this controller condition. The delay time was more than 200 ms, whereas it decreased remarkably to 40 ms after learning. The average error was also halved after learning. When IDM was pretrained, the delay time was about 50 ms from the first iteration. The average delay time slightly decreased after learning, whereas its variance was halved. The pretraining was more effective for decrease of the tracking error. The error decreased to $3.3 \pm 0.8°$ after learning, and it was less than 40% of the "pid." The average iteration number for all experiments were 23.5 for "random" and 5.8 for "pretrained" to reach minimum error.

Fig. 15 shows control performance when an external load was applied to the hand. The wrist angle was controlled three times with a 250 g cup in the hand. The controller was tuned under the load-free condition with the same subject. The amplitude in the response was short to the desired angle at the first iteration, probable because the weight of the controlled object increased. However, the control performance improved with a few iterations as seen in the graphs. This result demonstrated successful adaptation of the controller to the change in characteristics of controlled limbs. For slow movements, the controller will show good control performance from the first iteration under the loaded condition because the feedback component can compensate for the load and disturbance.

We concluded from these results that the proposed controller functioned as expected on FES experiments with the redundant musculoskeletal system for the tested sinusoidal trajectory. IDM was successfully learned during FES control and the FEL controller performed better than the conventional PID controller adjusted by the CHR method in terms of error evaluation and the delay time for the fast movement.
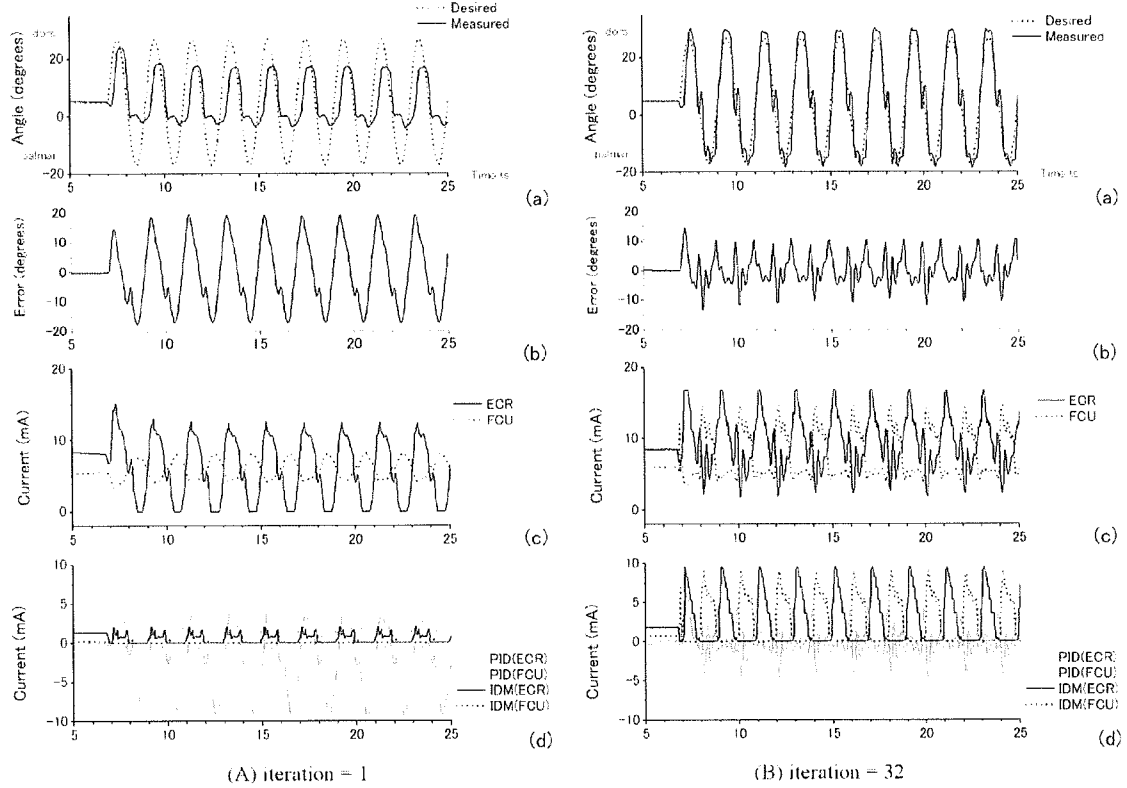
Fig. 11. Results of FES experiments (Subject F, random). Graphs show (a) the time course of the joint angle, (b) the tracking error, (c) the stimulus currents (S in Fig. 2), and (d) the outputs of each controller. Threshold of the stimulus current for ECR was 7.0 mA and that for FCU was 5.1 mA. Output range of S was 0–16.8 mA for ECR and 0–14.6 mA for FCU.
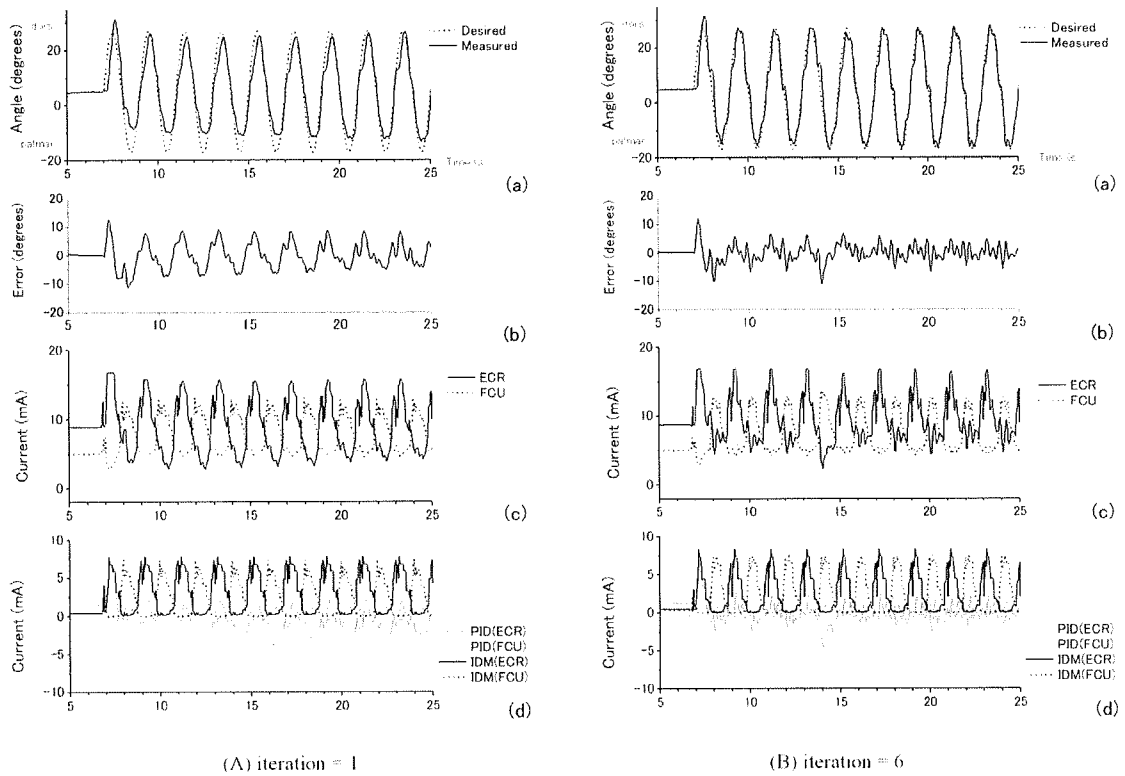

Fig. 12. Results of FES experiments (Subject F pretrained). Graphs show (a) the time course of the joint angle, (b) the tracking error, (c) the stimulus currents (S in Fig. 2), and (d) the outputs of each controller. Threshold of the stimulus current for ECR was 7.0 mA and that for FCU was 5.1 mA. Output range of S was 0–16.8 mA for ECR and 0–14.6 mA for FCU.

IV. DISCUSSION

The FEL scheme was introduced in the FES controller. The experimental results showed that adding the inverse dynamics model decreased the response delay to 40 ms even though the electrically stimulated musculoskeletal system had the latency of a hundred milliseconds and the time constant of a few hundred milliseconds. When multiple joints are controlled simul-
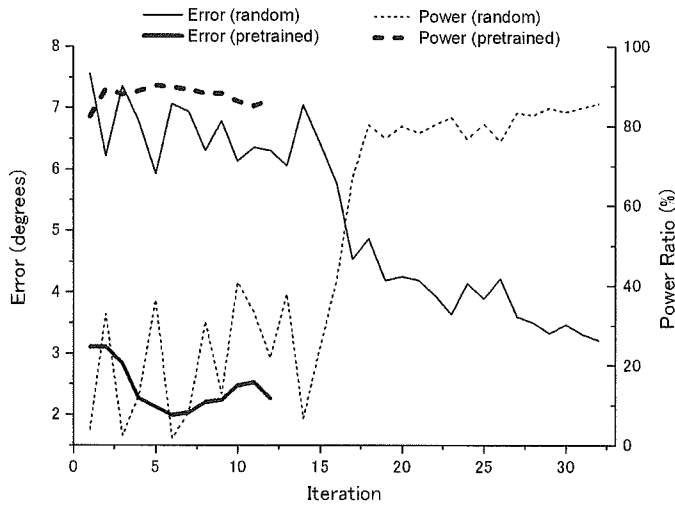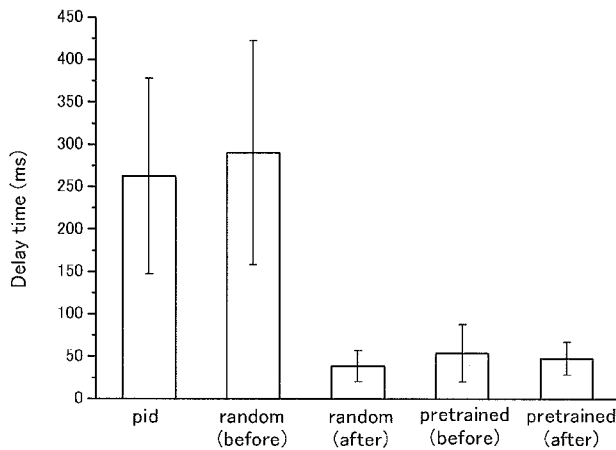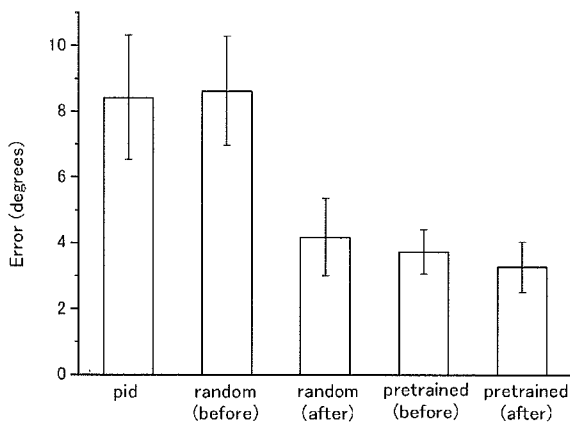
Fig. 13.　Change of the average error and the power ratio (Subject F). random: the initial connection weights in IDM were determined by a random number generator, pretrained: IDM was pretrained with the forward dynamics model in computer simulation. If the PID controller was used alone, the error was 8.9°.

(a) Average delay time

(b) Average error

Fig. 14.　Average delay time and average error of all FES experiments. "pid," "random," and "pretrained" represents the type of the controller. Here, "before" and "after" represents "before learning (First iteration)" and "after learning,"respectively. Average iteration number for all eight experiments were 23.5 for "random" and 5.8 for "pretrained."
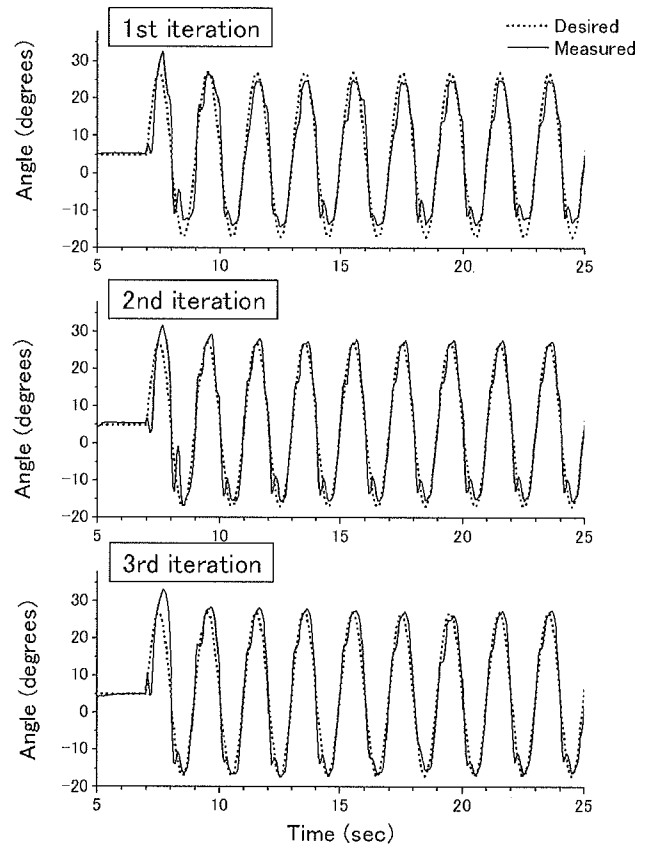

Fig. 15.　Control results with an external load (Subject A). Wrist angle was controlled three times with a 250 g cup in the hand. Controller was tuned under the load-free condition and applied to this loaded condition with the same controller parameters.

gait controls, control delay may cause patients to fall. Therefore, controllers that can control limbs with small delay hold great importance for FES control of paralyzed limbs. In addition, the burden caused by synthesis and regulation of stimulation patterns in clinical sites can be reduced with the proposed controller because IDM learns while controlling limbs. The adjustment of PID parameters is required before controlling limbs. However, these adjustment tasks cannot be burdensome for patients or medical staff because parameters are determined using only step and ramp responses as described. Those can be obtained automatically. Other prior measurements for obtaining characteristic of controlled limbs are not necessarily required for IDM learning.

This study used a four-layered neural network for the IDM. A general problem for using the neural network is its slow convergence of learning. These experimental results show that the network satisfactorily learned within a few dozen iterations for the tested ten-cycle reciprocating motion. Furthermore, only several iterations were required when IDM was pretrained with the artificial forward model. The required iteration number was inferred to be not large, even for use in clinical sites. Chang et al. [14] reported that 5000 training iterations were required to train their neuro-PID controller for one-muscle–one-DOF random movement of the knee. In addition, it must be noticed that the FEL controller can be used without learning for slow movements because the untrained controller is almost identical to the PID controller. However, we believe that further study

taneously (e.g., reaching movements), delay in one joint movement may yield failure in tracking accuracy of end effectors such as fingertips because of its kinematics. Moreover, considering

of the controller on other trajectories and on other joints is necessary for more precise evaluation. Not only layered neural networks, but also any other forms that are able to acquire inverse dynamics can be used for IDM. Therefore, other types of networks, such as radial basis function (RBF) neural networks [38] are candidates for the feedforward controller. From the viewpoint of additional learning ability, RBF is advantageous to the perceptron used in this study.

The average tracking error by our controller was $3.3 \pm 0.8°$ for 0.5-Hz movements. The tracking error for 0.5-Hz movements by the neuro-PID controller [14] was $5.32 \pm 1.44°$ on an able-bodied subject and $5.14 \pm 0.70°$ on a patient. The comparison between these controller performance is difficult because the FEL controller was evaluated on 2-muscle–1-DOF movement of the wrist, whereas the neuro-PID controller on 1-muscle–1-DOF movement of the knee. However, both controllers showed better control performance than single PID controller. Therefore, the hybrid arrangement is expected having high control performance. The advantages of the FEL scheme compared with other hybrid controllers are as follows: 1) ability to control redundant musculoskeletal systems; 2) pretraining of the feedforward controller (IDM) can be eliminated because it learns by itself while controlling limbs; and 3) the FEL controller can be used as a feedforward controller without sensors once IDM learning finishes.

Parameter optimization and pretraining using the artificial forward dynamics model facilitated the rapid learning of IDM. Development of the forward model and computer simulation offered great practical advantages for use of the controller. However, the forward model might not be a precise model of the subject's wrist in the FES experiments. Some inaccuracy might have been introduced into our study. For example, although the forward dynamics model was trained using the data obtained from Subject A, it was applied for the other subjects (Subjects B–F). As for Subject A, several days had passed after development of the model; the surface electrodes had been replaced. In addition, the forward model requires that each muscle had the same time constant of muscle activation. However, the iteration number that was required for IDM learning decreased remarkably by the pretraining of IDM. The results demonstrated that the use of the forward model, which might not be a perfect model of an individual person, was still quite effective for reducing the burdens of controller parameter tuning. Therefore, the following situation is anticipated if the FEL controller finds use in clinical sites: rough tuning of IDM is made with the standard forward dynamics model developed with data from a representative subject; thereafter, several iterations of fine-tuning are made for a specific patient. As described in the method chapter, such fine-tuning can be achieved while control. The controller learned and validated under the very specific condition (i.e., arm in the hanging position). Control performance will be degraded if the other joints, such as the elbow and the shoulder, are moved while controls because of the changes in muscle length and in the direction of the gravity. The angles of the other joints must be given into the model for varied conditions. Moreover, it is anticipated that IDM would acquire inverse dynamics within shorter iterations if the forward dynamics model was modified to allow different muscle activation dynamics.

In this paper, the controller was evaluated on two-muscle–one-DOF movement of the wrist. Our next research interest is the evaluation of the FEL controller on four-muscle–two-DOF movements (the dorsi/palmar-flexion and the radial/ulnar -flexion of the wrist). Development of the FEL controller for such a controlled object cannot be a difficult subject because our PID controller showed good performance on four-muscle–two-DOF movements [24]. However, some simplification methods must be proposed for developing the forward dynamics model of such controlled objects because the number of combinations of stimulation patterns for obtaining the input-output properties of musculoskeletal systems usually increases exponentially. A combination of neural networks and mathematical models may constitute a realistic approach to express forward models.

The tracking error converged and never decreased to $0°$ in all experiments and computer simulations even if learning–control activities were repeated more than several hundred times. The power ratio did not increase to 100%. These results show that IDM could not acquire accurate inverse dynamics of the controlled limbs. The reason is under investigation. However, it is thought that some technical limitations exist in the structure of IDM or in the feedback component. The control performance of the FEL controller is affected by the feedback controller because IDM refers to the feedback controller outputs for its learning. Therefore, improvement of the feedback component may contribute for more accurate FES control by the FEL controller. Other improvement can be an insertion of a low-pass filter in the controller. As shown in Fig. 10(a), quick motions were observed with the learned FEL controller. It is expected that smoother movements will be obtained if low-pass filters are inserted just after the FEL controller.

V. CONCLUSION

We studied a FES controller using the FEL scheme. The palmar/dorsi-flexion angle of the wrist was controlled by delivering stimuli to two muscles in the computer simulation and in FES experiments. Results showed that the FEL controller can learn within an acceptable number of iterations and that the controller performed better than the conventional PID controller that was adjusted by the CHR method for the tested fast movement, resulting decreased average tracking error and decreased response delay. Furthermore, the iteration can be decreased if the IDM is pretrained with the forward model of the controlled objects.

Further examination of the control system on other trajectories and on other joints is necessary. Extension of the controller and the experimental setup for controlling multiple DOF and multiple joint movements are our subjects for further study. Evaluation of the controller with actual patients is also necessary from a practical perspective. It is strongly hoped that joint-angle sensors that are easy to handle in clinical sites and are sufficiently accurate for use in a feedback controller can be developed for practical use.

REFERENCES

[1] P. E. Crago, P. H. Peckham, and G. B. Thrope, "Modulation of muscle force by recruitment during intramuscular stimulation," *IEEE Trans. Biomed. Eng.*, vol. BME-27, no. 12, pp. 679–684, Dec. 1980.

[2] S. A. Binder-Macleod, S. C. K. Lee, D. W. Russ, and L. J. Kucharski, "Effects of activation pattern on human skeletal muscle fatigue," *Muscle Nerve*, vol. 21, pp. 1145–1152, Sep. 1998.

[3] N. Hoshimiya, A. Naito, M. Yajima, and Y. Handa, "A multichannel FES system for the restoration of motor function in high spinal cord injury patients: A respiration-controlled system form multijoint upper extremity," *IEEE Trans. Biomed. Eng.*, vol. 36, no. 7, pp. 754–760, Jul. 1989.

[4] J. R. Buckett, P. H. Peckham, G. B. Thrope, S. D. Braswell, and M. W. Keith, "A flexible, portable system for neuromuscular stimulation in the paralyzed upper extremity," *IEEE Trans. Biomed. Eng.*, vol. 35, no. 11, pp. 897–904, Nov. 1988.

[5] N. Lan, H.-Q. Feng, and P. E. Crago, "Neural network generation of muscle stimulation patterns for control of arm movements," *IEEE Trans. Rehabil. Eng.*, vol. 2, no. 12, pp. 213–224, Dec. 1994.

[6] M. Rakos, B. Freudenshuβ, W. Girsch, C. Hofer, J. Kaus, T. Meiners, T. Paternostro, and W. Mayr, "Electromyogram-controlled functional electrical stimulation for treatment of the paralyzed upper extremity," *Arti. Organs*, vol. 23, pp. 466–469, 1999.

[7] M. M. Adamczyk and P. E. Crago, "Simulated feedforward neural network coordination of hand grasp and wrist angle in a neuroprosthesis," *IEEE Trans. Rehabil. Eng.*, vol. 8, no. 12, pp. 297–304, Sep. 2000.

[8] P. E. Crago, J. T. Mortimer, and P. H. Peckham, "Closed-loop control of force during electrical stimulation of muscle," *IEEE Trans. Biomed. Eng.*, vol. BME-27, no. 6, pp. 306–312, Jun. 1980.

[9] H. J. Chizeck, P. E. Crago, and L. S. Kofman, "Robust closed-loop control of isometric muscle force using pulsewidth modulation," *IEEE Trans. Biomed. Eng.*, vol. 35, no. 7, pp. 510–517, Jul. 1988.

[10] H. J. Chizeck, N. Lan, L. S. Palmieri, and P. E. Crago, "Feedback control of electrically stimulated muscle using simultaneous pulse width and stimulus period modulation," *IEEE Trans. Biomed. Eng.*, vol. 38, no. 12, pp. 1224–1234, Dec. 1991.

[11] T. Watanabe, T. Matsudaira, K. Kurosawa, T. Fujii, R. Futami, N. Hoshimiya, and M. Ichie, "Wrist joint control by multichannel closed-loop FES system: System improvement and first clinical test," in *Proc. 7th IFESS*, Ljubljana, Slovenia, 2002, pp. 265–267.

[12] M. A. Lemay and P. E. Crago, "Closed-loop wrist stabilization in C4 and C5 tetraplegia," *IEEE Trans. Rehabil. Eng.*, vol. 5, no. 9, pp. 244–252, Sep. 1997.

[13] M. Ianno, M. Ferrarin, A. Pedrocchi, and G. Ferrigno, "A neuro-adaptive control system for knee joint movements during quadriceps electrical stimulation," in *Proc. 7th IFESS*, Ljubljana, Slovenia, 2002, pp. 304–306.

[14] G.-C. Chang, J.-J. Luh, G.-D. Liao, J.-S. Lai, C.-K. Cheng, B.-L. Kuo, and T.-S. Kuo, "A neuro-control system for the knee joint position control with quadriceps stimulation," *IEEE Trans. Rehabil. Eng.*, vol. 5, no. 3, pp. 2–11, Mar. 1997.

[15] H. Qi, D. J. Tyler, and D. M. Durand, "Neurofuzzy adaptive controlling of selective stimulation for FES: A case study," *IEEE Trans. Rehabil. Eng.*, vol. 7, no. 6, pp. 183–192, Jun. 1999.

[16] P. H. Veltink, H. J. Chizeck, P. E. Crago, and A. El-Bialy, "Nonlinear joint angle control for artificially stimulated muscle," *IEEE Trans. Biomed. Eng.*, vol. 39, no. 4, pp. 368–380, Apr. 1992.

[17] M. Ferrarin, F. Palazzo, R. Riener, and J. Quintern, "Model-based control of FES-induced single joint movements," *IEEE Trans. Neural Syst. Rehabil. Eng.*, vol. 9, no. 9, pp. 245–257, Sep. 2001.

[18] A. Kostov, B. J. Andrews, D. B. Popovic, R. B. Stein, and W. W. Armstrong, "Machine learning in control of functional electrical stimulation systems for locomotion," *IEEE Trans. Biomed. Eng.*, vol. 42, no. 6, pp. 541–551, Jun. 1995.

[19] S. Jonic, T. Jankovic, V. Gajic, and D. Popovic, "Three machine learning techniques for automatic determination of rules to control locomotion," *IEEE Trans. Biomed. Eng.*, vol. 46, no. 3, pp. 300–310, Mar. 1999.

[20] B. T. Smith, M. J. Mulcahey, and R. R. Betz, "Development of an upper extremity FES system for individuals with C4 tetraplegia," *IEEE Trans. Rehabil. Eng.*, vol. 4, no. 12, pp. 264–270, Dec. 1996.

[21] L. J. Miller, P. H. Peckham, and M. W. Keith, "Elbow extension in the C5 quadriplegic using functional neuromuscular stimulation," *IEEE Trans. Biomed. Eng.*, vol. 36, no. 6, pp. 771–780, Jul. 1989.

[22] G. F. Wilhere, P. E. Crago, and H. J. Chizeck, "Design and evaluation of a digital closed-loop controller for the regulation of muscle force by recruitment modulation," *IEEE Trans. Biomed. Eng.*, vol. BME-32, no. 9, pp. 668–676, Sep. 1985.

[23] J. J. Abbas and H. J. Chizeck, "Neural network control of functional neuromuscular stimulation systems: Computer simulation studies," *IEEE Trans. Biomed. Eng.*, vol. 42, no. 11, pp. 1117–1127, Nov. 1995.

[24] T. Watanabe, K. Iibuchi, K. Kurosawa, and N. Hoshimiya, "A method of multichannel PID control of 2-degree of freedom of wrist joint movements by functional electrical stimulation" (in Japanese), *Trans. IEICE*, vol. J85-D-II, pp. 319–328, Feb. 2002.

[25] J.-J. J. Chen, N.-Y. Yu, D.-G. Huang, B.-T. Ann, and G.-C. Chang, "Applying fuzzy logic to control cycling movement induced by functional electrical stimulation," *IEEE Trans. Rehabil. Eng.*, vol. 5, no. 6, pp. 158–169, Jun. 1997.

[26] R. Davoodi and B. J. Andrews, "Computer simulation of FES standing up in paraplegia: A self-adaptive fuzzy controller with reinforcement learning," *IEEE Trans. Rehabil. Eng.*, vol. 6, no. 6, pp. 151–161, Jun. 1998.

[27] E. C. Sites and J. J. Abbas, "Sensitivity and versatility of an adaptive system for controlling cyclic movements using functional neuromuscular stimulation," *IEEE Trans. Biomed. Eng.*, vol. 47, no. 9, pp. 1287–1292, Sep. 2000.

[28] L. A. Bernotas, P. E. Crago, and H. J. Chizeck, "Adaptive control of electrically stimulated muscle," *IEEE Trans. Biomed. Eng.*, vol. BME-34, no. 2, pp. 140–147, Feb. 1987.

[29] H. Miyamoto, M. Kawato, T. Setoyama, and R. Suzuki, "Feedback-error-learning neural network for trajectory control of a robotic manipulator," *Neural Netw.*, vol. 1, pp. 251–265, 1988.

[30] M. Kawato, "Feedback-error-learning neural network for supervised motor learning," *Adv. Neural Comp.*, pp. 365–372, 1990.

[31] V. D. Kalanovic, D. Popovic, and N. T. Skaug, "Feedback error learning neural network for trans-femoral prosthesis," *IEEE Trans. Rehabil. Eng.*, vol. 8, no. 3, pp. 71–80, Mar. 2000.

[32] K. Kurosawa, R. Futami, T. Watanabe, and N. Hoshimiya, "Feedback error learning for controlling 1-DOF joint angle: Model simulation and experiment," in *Proc. 2003 IFESS*, Maroochydore, Australia, 2003, pp. 65–68.

[33] D. E. Rumelhart, G. E. Hinton, and R. J. Williams, "Learning representations by back-propagating errors," *Nature*, vol. 323, pp. 533–536, Oct. 1986.

[34] M. A. Arbib, *The Handbook of Brain Theory and Neural Networks*, 2nd ed. Cambridge, MA: MIT Press, 2002, pp. 21–22.

[35] K. L. Chien, J. A. Hrones, and J. B. Reswick, "On the automatic control of generalized passive systems," *Trans. ASME*, vol. 74, pp. 175–185, 1952.

[36] K. Kurosawa, H. Murakami, T. Watanabe, R. Futami, N. Hoshimiya, and Y. Handa, "A study on modification method of stimulation patterns for FES" (in Japanese), *Jpn. J. Med. Electron. Biol. Eng.*, vol. 34, pp. 103–110, Jun. 1996.

[37] K. Kurosawa, T. Watanabe, R. Futami, N. Hoshimiya, and Y. Handa, "Development of a closed-loop FES system using a 3-D magnetic position and orientation measurement system," *J. Autom. Control*, vol. 12, pp. 23–30, 2002.

[38] S. Chen, C. F. N. Cowan, and P. M. Grant, "Orthogonal least squares learning algorithm for radial basis function networks," *IEEE Trans. Neural Netw.*, vol. 2, no. 2, pp. 302–309, Mar. 1991.

[39] J. M. Hausdorff and W. K. Durfee, "Open-loop position control of the knee joint using electrical stimulation of the quadriceps and hamstrings," *Med. Biol. Eng. Comput.*, vol. 29, pp. 269–280, May 1991.

Kenji Kurosawa was born in Kawasaki, Japan, in 1971. He received the B.E. degree in electrical communication engineering, the M.E. degree in electrical and electrical communication engineering, and the Ph.D. degree in electronic engineering from Tohoku University, Sendai, Japan, in 1993, 1995, and 2004, respectively.

Since 1995, he has been with National Research Institute of Police Science, Japan, where he is a Senior Researcher in Physics Section, Second Forensic Science Division. His research interests are in the area of neuromuscular control by FES, image analysis, and electronic engineering for forensic science.

Dr. Kurosawa is a Member of the Institute of Electronics, Information and Communication Engineers (IEICE), the International Society for Optical Engineering (SPIE), the Japan FES Association, and Japanese Association of Forensic Science and Technology (JAFST).
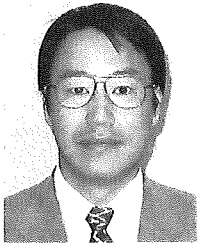
Ryoko Futami was born in Tochigi, Japan. He received B.E., M.E., and Ph.D. degrees in electronic engineering from the Tohoku University, Sendai, Japan, in 1980, 1982, and 1987, respectively.

From 1982 to 1988, he had been with the Hokkaido University, Sapporo, Japan, as a Research Associate. He is currently an Associate Professor in the Department of Electronic Engineering, Graduate School of Engineering, Tohoku University. His professional interests include the analysis and modeling of temporal pattern processing and higher-order functions in brain, and also the applied neuro-muscular control of paralyzed motor functions by FES.

Dr. Futami is a member of International Functional Electrical Stimulation Society (IFESS), Institute of Electronics, Information and Communication Engineers (IEICE), Japanese Society for Medical and Biological Engineering (JSMBE) and Japanese Neural Network Society (JNNS).

Takashi Watanabe (M'94) was received the B.E. degree in electrical engineering from Yamanashi University, Yamanashi, Japan, in 1989, and the M.E. degree in electrical and electrical communication engineering and Ph.D. degree in electronic engineering from Tohoku University, Sendai, Japan, in 1991 and 2000, respectively.

In 1993, he joined the staff of the Department of Electrical Communication Engineering, Tohoku University, as a Research Associate. Since 2001, he has been a Associate Professor at Information Synergy Center, Tohoku University. His research interests include neuromuscular control by FES, modeling of musculoskeletal system, and man–machine interface for paralyzed patients.

Dr. Watanabe is a Member the International Functional Electrical Stimulation Society (IFESS), the Japan Society of Medical Electronics and Biological Engineering (JSMBE), the Japan Society of Biomechanism, and the Japan FES Association.

Nozomu Hoshimiya (M'74–SM'90–F'94) was born in Japan, 1941. He received the Ph.D. degree in electronic engineering from Tohoku University, Sendai, Japan, in 1969.

From 1972 to May 1982, he was an Associate Professor in the Department of Electronic Engineering, School of Engineering, Tohoku University. From June 1982 to April 1988, he was a Professor in the Research Institute of Applied Electricity, Hokkaido University. Starting in May 1988, he was a Professor in Graduate School of Engineering, Tohoku University (Chair of Biomedical Electronics). He was a Vice-President of Tohoku University in 2001–2002. He has been the President of Tohoku Gakuin University since 2004. His principal fields of interest are the following biomedical engineering fields: functional electrical stimulation (FES) as a neural prosthesis, especially its application to rehabilitation fields; self-organizing neural networks, especially on the recognition and generation of the spatio-temporal patterns; and physiological instrumentation.

Dr. Hoshimiya was an Ad-Com Member of the IEEE/EMBS in 1989–1990, and was a founding Associate Editor of the IEEE TRANSACTIONS ON NEURAL SYSTEMS and REHABILITATION ENGINEERING, in 1993–1996. He was also an Editor-in-Chief of the *Journal of the Japan Society of Medical Electronics and Biological Engineering*, 1991–95. He has been an AIMBE Fellow since 2002. He was a Vice-President of the Japan Society of Medical and Biological Engineering in 1998–1999. He was a Member of the Board of Directors of the International Society of Functional Electrical Stimulation (FES) in 1999–2000, and has also been the President of Japan FES Society since 2004–2005.

機能的電気刺激（FES）制御法の開発におけるモデルシミュレーションの有用性：手関節制御での実験的検証

渡邉高志* 大塚雅幸** 上田智志** 吉澤 誠* 星宮 望***

* 東北大学情報シナジーセンター 仙台市青葉区荒巻字青葉6-6-05
** 東北大学大学院工学研究科 仙台市青葉区荒巻字青葉6-6-05
*** 東北学院大学 仙台市青葉区土樋1-3-1
nabe@isc.tohoku.ac.jp

要旨

脊髄損傷や脳卒中などによって生じた運動機能麻痺に対して，機能的電気刺激（FES）による運動機能再建が有効であることが臨床的に確認されてきた．その後，開ループ制御が中心である現在の制御方法に対して，閉ループ制御などの新しい制御手法の開発が望まれるようになってきた．FES制御法の研究開発においては，被験者での実験的検討が必要であるが，そのような実験的検討では，被験者に負担を生じたり，被験者間の違いや筋疲労などによって結果の再現性が低下したりする場合があって，研究遂行上の障害となっている．筋骨格モデルを用いた計算機シミュレーションは，被験者での実験的検討におけるそのような問題を解決可能であるので，FES制御法の研究開発において有効な研究手段になると期待される．そこで本研究では，FES制御法の研究開発において，被験者での実験的検討の一部に替わる研究手段としてモデルシミュレーションを利用することを検討している．そのため，電気刺激に対する非線形な応答特性を含めてFES研究に利用可能な上肢の筋骨格モデルを構築し，健常被験者での手関節2自由度運動のFES制御を対象として，計算機シミュレーション結果に関する実験的検証を行った．実験では，橈側手根屈筋（FCR），尺側手根屈筋（FCU），長／短橈側手根伸筋（ECRL/B），尺側手根伸筋（ECU）を表面電極で電気刺激して，手関節の掌背屈角度と橈尺屈角度の開ループ制御，および，閉ループ制御を行った．開ループ制御と閉ループ制御の結果から，計算機シミュレーションが，動作速度や上肢の肢位が異なる場合でも，健常被験者での実験結果をおおむね定性的に予測できることを確認した．いくつかの課題は残されているが，構築した筋骨格モデルによる計算機シミュレーションは，FES制御法の研究開発において，被験者での実験的検討の一部を代替する手法として有効になることが確認された．

機能的電気刺激(FES)による歩行制御法の開発のための筋骨格モデルの構築

◎柴田聡　　（東北大学大学院工学研究科）

渡邉高志（東北大学情報シナジーセンター）

Achmad　ARIFIN（東北大学大学院工学研究科）

吉澤誠　　（東北大学情報シナジーセンター）

星宮望　　（東北学院大学）

1．はじめに

　我々の研究グループでは，機能的電気刺激（FES）による歩行再建を目指して，Cycle-to-Cycle 制御に基づく片麻痺者の遊脚期の制御に着目してモデルシミュレーションによる検討を行ってきた [1]．これまでに，遊脚期の股・膝・足関節角度を制御するファジィ制御器を提案し，その有効性を示してきたが，遊脚期から立脚期への切り替えや立脚期の制御は検討していない．本研究では，立脚期も含めた FES による歩行再建を計算機シミュレーションで検討するため，筋骨格モデルと床面モデルを構築し，順動力学問題を解くことで接地の状態まで含めた FES 歩行の計算機シミュレーションについて検討を行った．

2．歩行モデルの構築

2－1．筋骨格モデル

　骨格モデルは，図1のように，遊脚の足，下腿，大腿，立脚の大腿，下腿の5つのセグメントと，それらを連結する左右の足関節と膝関節，股関節から構成した．なお，全ての関節は矢状面内のみに可動域を持つ蝶番関節とした．また，対象を歩行中の下肢に限定し，左右対称であること，立脚期にある足は動作を通して地面に固定であることを仮定した．頭部や体幹，上肢は1つの質点で表現し，その全質量を股関節上に集中させた．各セグメントの質量は，セグメントの中央に1つの質点として集中させた [2]．関節トルクの符号は，全て反時計回りを正とした．セグメントの質量や長さなどのパラメータ値は文献 [3] を用いた．

　関節トルク（τ）は，電気刺激によるトルク（τ_{CE}）と受動粘弾性要素によるトルク（τ_P）の和として次式で求めた [4]．

$$\tau = \tau_{CE} + \tau_P \qquad (1)$$

　τ_{CE} は，電気刺激により発生する筋収縮力 F_{CE} とモーメントアーム（固定）との積により求められ，F_{CE} は，筋の活動度，長さ-張力関係 [5]，収

縮速度-張力関係 [6]，最大筋張力 F_{max} で表される Hill 型モデルにより求めた．なお，電気刺激による筋の活動度は，刺激強度に対する筋のリクルートメント特性 [7] と活性化ダイナミクス [8] により求めた．受動粘弾性要素によるトルク（τ_P）は，各関節での運動毎に（2）式で記述し [9]，これにより関節可動域も表現した．

$$\tau_p = -k_{i1}\exp\{k_{i2}(\theta_i + k_{i3})\} \\ + k_{i4}\exp\{-k_{i5}(k_{i6} + \theta_i)\} - c_i\dot{\theta}_i \qquad (2)$$

ここで，$k_{i1} \sim k_{i6}$ および c_i は，関節毎に異なる係数である．

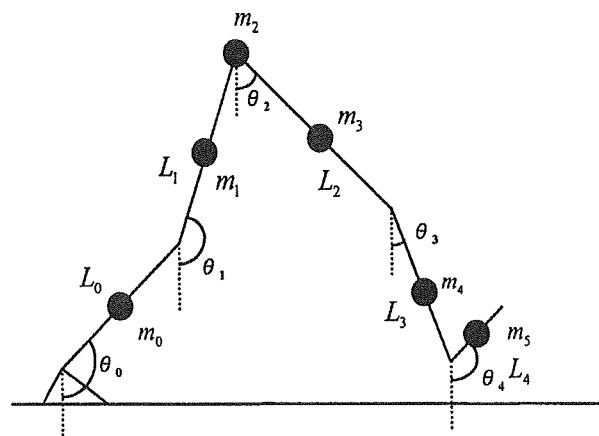　運動方程式は Lagrange 法により導出した．モデルに使用した筋は，各関節での各運動における主動筋となるものを選択した（表1）．

図1　骨格モデル（$\theta_0 \sim \theta_4$：鉛直方向からの振れ角，$L_0 \sim L_4$：各セグメント長，$m_0 \sim m_4$：各セグメント質量を集中させた質点）

表1　モデルに含まれる筋とその作用

主動筋	作用
ヒラメ筋（Sol）	足関節の底屈
前脛骨筋（TA）	足関節の背屈
腓腹筋（Gas）	足関節の底屈，膝関節の屈曲
大腿直筋（RF）	股関節の屈曲，膝関節の伸展
広筋群（Vas）	膝関節の伸展
ハムストリングス（大腿二頭筋短頭・大腿二頭筋長頭）(Ham)	股関節の伸展，膝関節の屈曲
腸腰筋（IL）	股関節の屈曲

2-2. 床面モデル

床面モデルは，作用点に働く力の x 成分 f_g^x と y 成分 f_g^y を（3）式で表現した[9]．

$$f_g^x = \begin{cases} -k^G(x_g - x_g^0) - c^G \dot{x}_g & (y_g \leq 0) \\ 0 & (y_g > 0) \end{cases}$$

$$f_g^y = \begin{cases} -k^G y_g + c^G f_{max}(-\dot{y}_g) & (y_g \leq 0) \\ 0 & (y_g > 0) \end{cases} \quad (3)$$

$$f_{max}(x) = \max(x, 0)$$

ここで，k^G，c^G は係数，x_g，y_g は床反力作用点位置，x_g^0 は接地した瞬間の水平方向の作用点位置であり，踵とつま先に床面モデルを付けた．図1のモデル構造を基に，踵への床反力の作用点は足関節部とし，踵とつま先への床反力が作用し始める高さを立脚の足関節位置に一致させた．このモデルによって得られた床反力を（4）式により等価関節トルクに変換した[10]．

$$\tau = J^T F \quad (4)$$

ここで τ は各関節トルクのベクトル，J はヤコビ行列，F は作用点に働く力のベクトルである．

3. 計算機シミュレーション
3-1. 方法

前述の筋骨格モデルを利用し，ファジィ制御を用いた Cycle-to-Cycle 制御による遊脚期の制御[1]に関する計算機シミュレーションを行った．片麻痺者を想定しているため，立脚の各関節角度は常に健常者の歩行における関節角度軌跡と一致させ，遊脚の各関節角度の初期値も健常者の歩行における対応する関節角度と一致させた．Cycle-to-Cycle 制御では，電気刺激パルス列を印加する時間 TB[s] を調整し，遊脚期における重要な点での角度を制御する．目標角度は，健常者の歩行の遊脚期における股関節の最大屈曲角度と最大伸展角度，膝関節の最大屈曲角度と最大伸展角度，足関節の最大背屈角度と最大底屈角度，遊脚期の最終姿勢（着床）における各関節の角度とした[1]．計算機シミュレーションの時間ステップは 10^{-6}[s] とし，制御結果は 20[ms] ごとに測定した．微分方程式の解法として 4 次のルンゲクッタ法を用いた．

最初に，これまでの研究[1]と同様に，遊脚期のみの制御について，各筋の TB[s] の初期値を 0[s] として 50 歩分のシミュレーションを行った．被刺激筋は表1の通りである．

次に，遊脚期の終了から，足部が床面に接する状態までの計算機シミュレーションを行った．遊脚期制御の最終姿勢によっては床反力が生じない場合があるため，遊脚期の制御の終了から遊脚の足関節部に床面モデルが作用するまでの立脚の足関節角度，膝関節角度を試行錯誤的に決定し，立脚側を動作させた．また，麻痺側の着床後の足部が床面に平らになる現象を見るためつま先の床面モデルは作用しないものとした．

最後に，遊脚期から立脚期への切り替えに関する計算機シミュレーションを試みた．遊脚の足部が床面とほぼ平行になった時点で遊脚の足部が固定されて立脚に切り替わることとし，その時点での立脚と遊脚の各関節の角度，角速度を切り替え後の遊脚と立脚のそれぞれの初期値とした．なお，床反力は切り替え後の遊脚に作用するものとし，麻痺側（立脚）には電気刺激を与えず，また健側（遊脚）も床面モデルから力を受けるものの能動的な力を出さないようにして計算機シミュレーションを行った．

3-2. 結果

最初に，遊脚期のみの FES 制御による結果について，図2に各関節角度の軌跡，図3に stick picture，図4に得られた電気刺激バーストパターンを示す．図2と図3の結果は先行研究の結果と同様であったが，図4については，TA と Sol への電気刺激は印加されなかった．先行研究での電気刺激スケジュールにおいて足関節の最大背屈位から最終姿勢（着床）に向けて，TA と Sol への電気刺激の印加は必要であったが，本モデルを用いた結果では，着床時の足関節の角度誤差が非常に小さくなったため不要になったと思われる．

次に，図4の刺激バーストパターンによる制御が終了した後，着床する状態についてのシミュレーション結果を図5に示す．図5(a)では，床面モデルが無いために，遊脚期の終了時点での運動の影響を受けて股関節が屈曲し続け，膝関節が伸展位を維持している．図5(b)では，床面モデルの作用により遊脚の股関節，膝関節が屈曲している．しかし，ここでの結果では，踵が着床した後，足関節の底屈が生じなかったため，遊脚期の最後に足関節が底屈するような電気刺激（図6）を与えた．これによる制御結果

が図5(c)である.

最後に,床面に接した後に脚の切り替えを行った結果を図7に示す.脚の切り替え後は,麻痺側には電気刺激を与えず,また健側も床面モデルから力を受けるものの能動的な力を出さないようにしたため,切り替え後に両膝関節が屈曲していく結果となった.

4.考察

ファジィ制御による Cycle-to-Cycle 制御の結果は,ほぼ先行研究と同様であり,床反力の作用や麻痺側の遊脚から立脚への切り替え後の転倒の様子から,構築されたモデルは妥当であると考えられる.しかし,遊脚期の制御においては,本来ならば,遊脚期の最終姿勢で踵が着床するはずであるが,今回のシミュレーション結果では着床が起こらなかった.健常者の歩行に
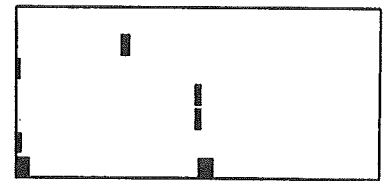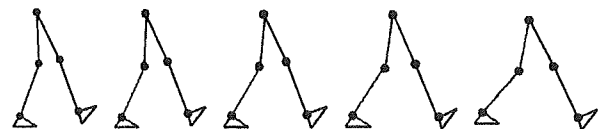

図2　各関節の角度軌跡.股関節角度:鉛直方向から屈曲方向を正,膝関節角度:大腿部の延長線と下腿部の為す角について屈曲方向を正,足関節角度:足部の甲と下腿部の延長線が為す角について90°を0°として屈曲方向を正としてプロットした.

図3　遊脚の制御の様子(遊脚期の 200ms 毎のstick picture. 黒:モデル,灰:健常者)

図4　遊脚期を適切に再建する電気刺激バーストパターン(1:遊脚開始,2:足関節最大底屈,3:膝関節最大屈曲,4:股関節最大屈曲,5:遊脚終了)

(a)　床面モデル無し,底屈電気刺激無し

(b)　床面モデル有り,底屈電気刺激無し

(c)　床面モデル有り,底屈電気刺激有り

図5:着床後 150ms 毎の stick picture(黒:麻痺側,灰:健側)
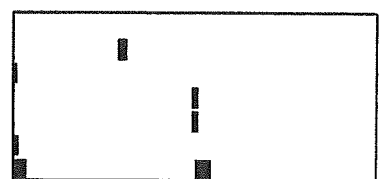
図6　適切な着床で制御するための電気刺激バーストパターン
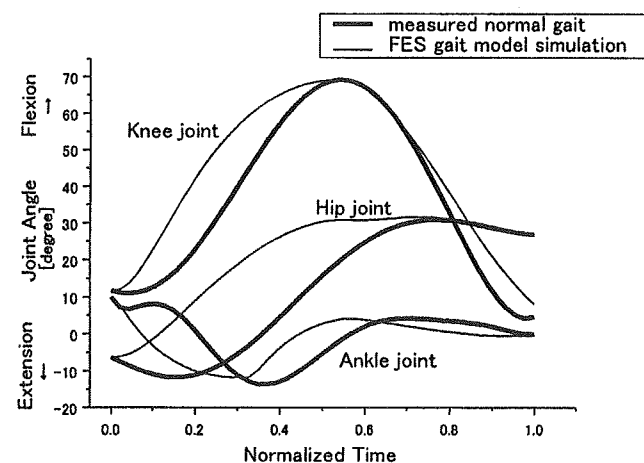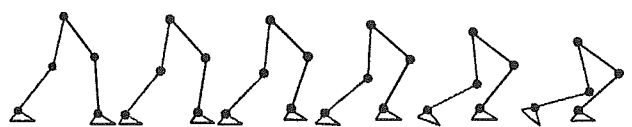

図7　麻痺脚を遊脚から立脚へ切り替えた後のシミュレーション結果(脚の切り替え後 25ms毎の stick picture. 黒:麻痺側,灰:健側)

おいて，立脚の踵やつま先は床面から離れるが，本モデルの立脚の足部は常に地面に固定としたため，股関節の位置に誤差が生じたことが原因であると思われる．また，床反力を等価関節トルクに変換するが，脚の切り替えにより足部が固定されると床面モデルの作用が終了するので，切り替え後の初期値には，各関節の等価関節トルクを与えていない．これも，立脚の足を床面に固定したことで生じた検討課題である．今後，立脚期の FES 制御法を開発する上で本モデルを用いることの妥当性を，FES 制御法とモデル構造の両面から検討する必要がある．さらに，着床時に麻痺側の足部が床面に接するための底屈が現れなかったこと，床面モデルの出力値を評価していないことから，モデルパラメータ値の検討も必要である．

5．まとめ

本報告では，歩行の FES 制御法の開発に利用することを目的とした筋骨格モデルと床面モデルの構築を行った．このモデルを用いて，これまでの遊脚期のみの制御から立脚期も含めた制御のシミュレーションに拡張するための検討を行った．遊脚期の制御では先行研究と類似した結果が得られ，床反力の作用や，遊脚から立脚への切り替え後の結果から，本モデルがおおむね妥当であり，本モデルを用いて一定の歩行状態を表現できると思われる．今後は，FES 制御法の検討に本モデルを用いることの妥当性を，FES 御法とモデル構造の改良の必要性の両面から検討していく予定である．

参考文献
1) A. Arifin, T. Watanabe, M. Yoshizawa, N. Hoshimiya : "A test of fuzzy controller of cycle-to-cycle control for controlling three-joint movements of swing phase of FES gait," 第 25 回バイオメカニズム学術講演会予稿集，pp.43-46, 2004

2) M.G.Pandy, N. Berme : "A numerical method for simulating the dynamics of human walking," J.Biomechanics, 21(12), pp.1043-1051, 1988

3) N. Ogihara, N. Yamazaki : "Generation of human bipedal locomotion by a bio-mimetic neuro-musculo-skeletal model," Biol. Cybern., 84, pp.1-11, 2001

4) 渡邉高志，帖佐征一，吉澤誠，星宮望："機能的電気刺激（FES）による麻痺上肢制御法の開発における筋骨格モデルの利用"，第 19 回生体・生理工学シンポジウム論文集，pp.135-138, 2004

5) BM. Nigg, W. Herzong : "Biomechanics of the Musculo-skeletal system," John Wiley & Sons, Inc., 1995

6) GM. Eom, T. Watanabe, R. Futami, N. Hoshimiya, Y. Handa : " Computer-aided generation of stimulation data and model identification for functional electrical stimulation (FES) control of lower extremities," Frontiers Med. Biol. Engng, 10(3), pp.213-233, 2000

7) M. Vevy, J. MIzrahi, Z. Susak : "Recruitment, force and fatigue characteristics of quadriceps muscles of paraplegics isometrically activated by surface functional electrical stimulation, " J.Biomed.Engng, 12, pp.150-156, 1990

8) M.G. Pandy, B.A. Ganer, C. Anderson : " Optimal control of non-ballistic muscular movements- a constraint-based performance criterion for rising from a chair," J. Biomech. Engng, 37, pp.15-26, 1995

9) 長谷和徳，山崎信寿："神経振動子と遺伝的アルゴリズムを用いた実 2 足歩行類似運動の生成"，計測自動制御学会論文集，33(5), pp.448-454,1997

10)日本ロボット学会："ロボット工学ハンドブック"，コロナ社，pp.214-216，1990

....

980-8579 仙台市青葉区荒巻字青葉 6-6-05
東北大学大学院工学研究科電気・通信工学専攻
吉澤研究室　　柴田　聡
TEL:022-795-7130　FAX:022-263-9163
E-mail:shibata@yoshizawa.ecei.tohoku.ac.jp

経皮的電気刺激による皮膚感覚を用いたパターン提示に関する基礎的検討

◎ 佐藤　由規 （東北大学大学院工学研究科）

渡邉　高志 （東北大学情報シナジーセンター）

吉澤　誠 （東北大学情報シナジーセンター）

星宮　望 （東北学院大学）

1．はじめに

皮膚感覚は視覚や聴覚に代わる情報伝達の手段として重要であり，例えば，義肢や機能的電気刺激（FES）を使用する場合には，制御の命令や状態を使用者に示す際に有効になる．これには，機械的な振動を用いる方法と電気刺激を用いる方法がある．本研究では，電気刺激により生じる感覚を用いて情報提示を行う手法に着目する．

梶本ら [1] は指先に装着した電極で電気刺激感覚を提示する触覚ディスプレイを提案している．この手法では，指先を覆ってしまうため，手を使う作業での情報提示への応用は困難である．また，触覚を提示するのに最も適した部位は指先であると言われているが [2]，義肢使用者や麻痺患者に関しては，残存する手指などは他の用途や装置の操作等に使用するため，提示部位として適切とは言えない．一方，金ら [3] は，前腕に電極を配置して，電気刺激パターンをある単語に結びつけて情報の伝達を行なう方式を提案している．この手法は，刺激パターンを単語と対応させるため，提示するパターン数を多くできないといった課題が挙げられる．

本研究では，単語や意味情報を直感的に与えることに着目し，装置操作や作業の妨げとならない前腕部を提示部位として，文字のようにそれ自体に意味のある情報を皮膚電気刺激感覚により提示する方法を検討する．本報告では，最初に，2点の電気刺激感覚に対する識別能力を調べ，情報を提示する電気刺激パターンを印加する電極の構造を検討した．次に，マトリックス状に配置した電極を用い，電気刺激を印加する電極を変えることで生じる移動感覚によりパターンを提示する方法を検討した．

2．2点の電気刺激感覚の識別

2．1　実験方法

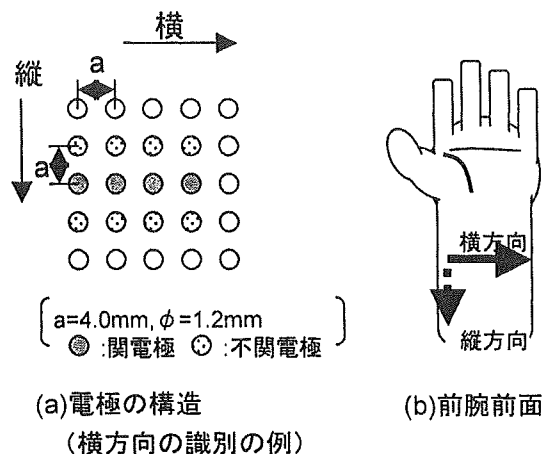図1に示す5×5のマトリックス状の表面電極（電極直径 1.2mm のステンレス線，電極の中心間距離 4.0mm）を製作し，横1列または縦1列に並んだ4つの電極を関電極として使用し，その上下または左

図1．2点の電気刺激感覚の識別で使用した電極と刺激部位の概要

右の電極を各関電極に対する不関電極として電気刺激を与えた．刺激パルスは，パルス幅 $200\mu s$，パルス周波数 100Hz の単相性矩形波 [4] をパーソナルコンピュータで作成し，刺激装置により定電圧刺激として出力した．

健常被験者6名（男性5名，女性1名）に対し，左前腕前面の中央付近に導電性ペーストを塗付した電極を装着し，横方向と縦方向について2点の電気刺激感覚の識別能力を測定した．最初に，各刺激電極の刺激閾値及び刺激の最大値（痛みや不快感を感じ始める刺激強度）を測定し，その後被験者が判断しやすい刺激強度を設定した．識別実験では，4つの電極のうち1つに電気刺激を1s間印加し，1sの休止時間を挟んで4つのうちのどれか1つの電極へ再び1s間刺激を印加した．1回の測定セットは，順序の違いを含めた4つの異なる電極の組み合わせ24種と同じ電極の組み合わせ4種の計28種について，2回の刺激電極が同じかどうかを回答させた．刺激を印加する電極の組み合わせはランダムに決定し，横方向と縦方向に対してそれぞれ2セットずつ実験を行った．

2．2　結果

表1に電極間距離ごとの正答率を示す．これより，隣接する電極（電極間距離 4mm）に対する識別能力

表1．2点の電気刺激感覚の識別結果

被験者	横方向の正答率(%)			縦方向の正答率 （%）		
	4mm	8mm以上	全体	4mm	8mm以上	全体
A	75.0	91.7	83.3	62.5	91.7	77.1
B	91.7	100.0	95.8	91.7	87.5	91.7
C	83.3	91.7	79.2	83.3	87.5	83.3
D	45.8	83.3	79.2	75.0	79.2	77.1
E	70.8	100.0	79.2	58.3	95.8	77.1
F	75.0	75.0	58.3	50.0	75.0	62.5

$a=8mm, b=1.2mm, \phi=1.2mm$
◎:関電極　▨:不関電極

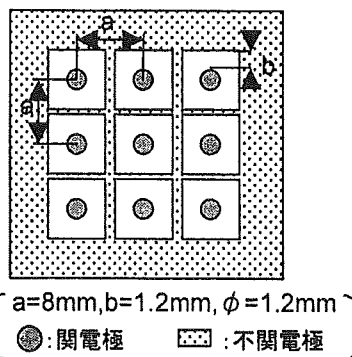図2．パターン認識実験で使用した電極

は被験者ごとに差が大きくなったが，電極間距離が8mm以上の場合には，ほとんどの被験者が高い正答率を示した．そこで，パターン認識の実験では，電極間距離を8mmに設定した．

3．パターン認識実験

3．1　実験方法

前述の結果をもとに，電極の中心間距離を8mmとして，3×3のマトリックス状の電極を製作した（図2）．製作した表面電極は，ステンレス製の関電極（直径1.2mm）の周りに正方形の溝を作り絶縁し，その周囲を銅製の不関電極とした．関電極と不関電極の間隔は最短で1.2mmとなっている．

前述と同じ健常被験者6名（男性5名，女性1名）で，導電性のペーストを塗付した表面電極を被験者の左前腕前面の中央付近に装着し，電気刺激パターンによる認識実験を行った．被験者に提示する刺激パターンは図3に示す16種類で，大きく二つのグループに分かれる．A群は提示時間約1s（1個の電極の提示時間0.33s）となる刺激パターン8種で，1本の線上を点刺激が移動するパターン（[1]～[6]），2本の線上を同時に移動するパターン（[7], [8]）である．B群は提示時間約1.8sとなる刺激パターン8種で，2本の線上を順に移動するパターン（[9], [10]），1本の線上を往復するパターン（[11], [12]），L字やV字の軌跡を移動するパターン（[13]～[16]）である．被験者にはこれらのパターンをランダムな順に提示し，知覚されたパターンの番号を，図3を見ながら回答させた．

2章と同様に，最初に全ての刺激電極について被験者が判断しやすい刺激強度を設定した．次に，16種類のパターンをそれぞれ2回ずつ提示して，提示パターンと知覚されたパターンとの対応を教示した後，各パターンを5回ずつ，計80回をランダムな順に提示してパターン認識の訓練を行った．この時，被験者には各回答後に正解を示した．その後，パタ
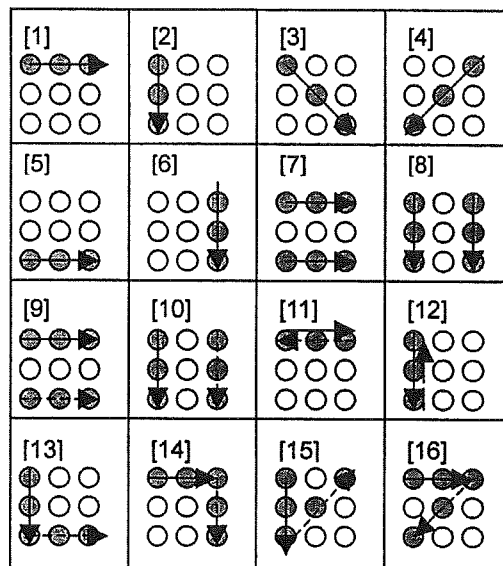

図3．パターン認識実験で用いた提示パターン

ーン認識実験を行った．1回の認識実験では，図3の16種類のパターンを5回ずつ，計80回をランダムな順に提示し，知覚されたパターンの番号を，図3を見ながら回答させた．各被験者に対し，1日に2セット，3日間で計6セットの認識実験を行った．

3．2　結果

図4に3日間の被験者毎の正答率の推移を示す．初日に比べ3日目の方が正答率が上昇する傾向がみられ，被験者数が少ないものの1日目と3日目の正答率に有意差があった（一標本t検定，p<0.05）．この結果を踏まえ，3日目の実験結果について解析を行った．

表2に3日目の各提示パターンの正答率を示す．これより，パターン[2]，[4]，[6]は4名以上の被験者で70%以上の正答率が得られており，比較的認識し易いパターンであるといえる．一方，パターン[3]，[7]，[15]は4名以上の被験者で正答率が30%以下と低くなっており，他の提示パターンと間違えやすいパターンであると考えられる．